NASA-CR-152,344

NASA CONTRACTOR REPORT 152344

NASA-CR-152344
19830003829

Hybrid LTA Vehicle Controllability As Affected By Buoyancy Ratio

Donald N. Meyers
Piotr Kubicki
T. Tarczynski
A. Fairbanks
F. N. Piasecki

LIBRARY COPY

FEB 9 1982

LANGLEY RESEARCH CENTER
LIBRARY, NASA
HAMPTON, VIRGINIA

CONTRACT NAS2– 10185
October 1979

NASA

ENTER:ENTER;D 83N12099
DISPLAY 83N12099/2
83N12099*# ISSUE 3 PAGE 328 CATEGORY 8 RPT#: NASA-CR-152344 NAS
1.26:152344 PIAC-97-C-6 CNT#: NAS2-10108S 79/10/00 63 PAGES
UNCLASSIFIED DOCUMENT
UTTL: Hybrid LTA vehicle controllability as affected by buoyancy ratio TLSP:
Final Report
AUTH: A/MEYERS, D. N.; B/KUBICKI, P.; C/TARCZYNSKI, T.; D/FAIRBANKS, A.;
E/PIASECKI, F. N.
CORP: Piasecki Aircraft Corp., Philadelphia, Pa. AVAIL.NTIS SAP: HC A04/MF
A01
MAJS: /*BUOYANCY/*CONTROLLABILITY/*HEAVY LIFT AIRSHIPS/*LOW SPEED STABILITY/*
WIND (METEOROLOGY)
MINS: / ACCELERATION (PHYSICS)/ AEROSTATICS/ HORIZONTAL ORIENTATION/ INFLATABLE
STRUCTURES/ ROCKET ENGINES
ABA: S.L.
ABS: The zero and low speed controllability of heavy lift airships under
various wind conditions as affected by the buoyancy ratio are
investigated. A series of three hybrid LTA vehicls were examined, each
having a dynamic thrust system comprised of four H-34 helicopters, but
with buoyant envelopes of different volumes (and hence buoyancies), and
with varying percentage of helium inflation and varying useful loads
(hence gross weights). Buoyancy ratio, B, was thus examined varying from
approximately 0.44 to 1.39. For values of B greater than 1.0, the dynamic
MORE ENTER:

NASA CONTRACTOR REPORT 152344

Hybrid LTA Vehicle Controllability As Affected By Buoyancy Ratio

Donald N. Meyers
Piotr Kubicki
T. Tarczynski
A. Fairbanks
F. N. Piasecki
Piasecki Aircraft Corporation
Island Rd., International Airport
Philadelphia, Pennsylvania 19153

Prepared for
Ames Research Center
under Contract NAS2-10185

National Aeronautics and
Space Administration

Ames Research Center
Moffett Field, California 94035

N83-12099#

TABLE OF CONTENTS

1. SUMMARY

An analytical investigation was made of the low-speed controllability of the Piasecki "Heli-Stat" concept of heavy-vertical-lift hybrid lighter-than-air (LTA) vehicles, particularly as affected by buoyancy ratio. A matrix of designs was studied based upon a helium-filled ellipsoidal aero-stat supporting a rigid structural space frame which interconnects four SH-34J helicopter rotor/propulsion systems. The tail rotor of each helicopter was considered to be removed and replaced by a ducted propeller capable of absorbing full engine power, with deflecting vanes to vector the propeller thrust laterally in addition to its normal forward thrust. The geometric arrangement of the four helicopter systems and their interconnecting frame was kept unchanged. The aerostat, however, was varied in overall displaced volume, and also in percentage of helium inflation. As in normal LTA practice, the displaced volume not filled with helium consists of air in internal ballonets.

Three sizes of aerostat were examined, ranging from 21,200 m^3 (750,000 ft^3) to 42,500 m^3 (1,500,000 ft^3) displacement. Each volume was studied with helium inflation of 86.2% and 95%, representing a ballonet ceiling (altitude at which all air in the ballonets is exhausted) of 1,520 m (5,000 ft.) and 520 m (1,700 ft.), respectively. All maneuvers, however, were assumed to be performed at standard sea-level conditions, 15°C (59°F) and 760 mm (29.92 in.) of mercury. Various useful loads were also assumed for each configuration, varying from minimum flying weight to a weight requiring maximum rated thrust from the SH-34J rotors. The resulting matrix of configurations gave a range of buoyancy ratios from approximately 0.44 to 1.39.

The ability to produce horizontal forces in all directions independently of the main rotors contributes significantly to controllability under conditions of near neutral buoyancy. Because of this feature controllability becomes relatively insensitive to buoyancy ratio (defined as static lift divided by total lift). When operating at near-neutral buoyancy, the auxiliary thrusters become the primary control means. As buoyancy ratio departs from a value of 1.0, either higher or lower, the importance of lateral thrusters decreases.

1. (Cont'd)

The ability to roll the vehicle increases the available vectoring angle of the lifting thrusters and increases significantly the ability to trim and accelerate in a crosswind. For buoyancy ratios greater than 1.0, however, the control coupling between roll and thrust vectoring must be reversed, since the thrust is downward instead of upward. Thus the vehicle is made to roll "out of the wind" instead of "into the wind".

Aerostat size has an important effect on acceleration capability particularly in yaw, because of the dominant effect of increasing moment of inertia. The largest configuration examined, which has twice the volume of the smallest, has 30% as much acceleration capability at 0° or 90° sideslip angle, decreasing to 10% at 40° to 60°. Nevertheless, even this latter 42,500 m^3 (1,500,000 ft^3) size is far more maneuverable than the older generation LTA's, and is calculated to be able to maneuver against a 20-degree crosswind of up to 11 m/s (22 knots).

The results of this study should be considered preliminary because of the simplified analysis. Although the X- and Y- components of total drag in a side-slip as well as the aerodynamic yawing moment were included, the sideward "lift" force acting on the aerostat was not. Thus the calculated lateral acceleration capability in a crosswind is somewhat high. A calculation of the 28,300 m^3 (1,000,000 ft^3) vehicle with the "lift" force included showed that the reduction in maximum trimmable crosswind speed ascribable to this effect was of the order of two knots, and occurred at sideslip angles in the vicinity of 40 degrees.

Another aspect to be considered is that the aerostat shape is aerodynamically unstable in pitch and yaw without tail surfaces, which were assumed to be absent. However, stability characteristics were beyond the scope of effort, and were not included. Without stabilizing control margins to provide adequate dynamic handling qualities, operations to combinations of sideslip angles and speeds would be less than the values indicated herein.

2. LIST OF FIGURES

3. LIST OF TABLES

4. INTRODUCTION

Hybrid lighter-than-air (LTA) vehicles (semi-buoyant) appear to be an excellent solution for the mission of very heavy vertical air lift. Designs have been postulated in studies by Piasecki Aircraft Corp. (PiAC) capable of payloads over 150 tons.

For many heavy vertical lift applications it is necessary to place the payload accurately in position from the hovering LTA vehicle. Thus low-speed controllability becomes an important characteristic. Ref. 6 is a parametric study performed by PiAC, of the effects on controllability of the major geometric and dynamic variables, namely the magnitude and spacing of the thrusters (rotors). This magnitude of the required vertical thrusters, in a given case, is a function of the buoyancy ratio, β, defined as the ratio of static (buoyant) lift to gross weight.

This report constitutes an investigation of the zero- and low-speed controllability of heavy-lift airships under various wind conditions as affected by the buoyancy ratio. A series of three hybrid LTA vehicles were examined, each having a dynamic-thrust system comprised of four H-34 helicopters, but with buoyant envelopes of different volumes (and hence buoyancies), and with varying percentage of helium inflation and varying useful loads (hence gross weights). Buoyancy ratio, β, was thus examined varying from approximately 0.44 to 1.39. For values of β greater than 1.0, the dynamic thrusters must supply negative thrust (i.e. downward).

5. METHOD OF ANALYSIS

5.1 DESCRIPTION OF HELI-STAT VERSIONS

The type of hybrid LTA vehicle analyzed herein is the Piasecki Heli-Stat, which is comprised of an aerostat, to which is attached a multiplicity of helicopter rotors to provide dynamic lift, propulsion, and control.

In this study the dynamic system consists of four SH-34J helicopters arranged symmetrically in a rectangular pattern, two on either side of an ellipsoidal helium aerostat, as shown in Fig. 1. The helicopters are attached to an interconnecting structure which, in turn, is connected to an aerostat. In order to investigate the effects of buoyancy ratio on controllability three different sizes of aerostat have been examined, with displaced volumes of 21,200 m^3 (750,000 ft^3), 28,300 m^3 (1,000,000 ft^3) and 42,500 m^3 (1,500,000 ft^3). The dimensional arrangement of the helicopters, however, has been kept constant for all three Heli-Stat sizes. Dimensions pertinent to the analysis are given in Fig. 1.

A matrix of study versions was created as follows. Each of the three aerostat volumes is inflated, at sea level standard atmosphere, either 86.2% or 95.0% with helium (of 95% purity). The remainder of the displaced volume consists of air in the ballonets. Each size is then analyzed at several loading conditions, varying from minimum flying weight to maximum gross weight as limited by the allowable rotor thrust of the SH-34J rotors. This allowable thrust is assumed to be the maximum allowable gross weight of the SH-34J helicopter (operating as a normal separate helicopter), which is 57.8 kN (13,000 pounds force). In some instances minimum flying weight is less than the buoyant lift of the aerostat (buoyancy ratio, β, is greater than one). In such an event the particular case of neutral buoyancy ($\beta = 1.0$) is also considered. Table 1 lists the individual configurations analyzed.

The SH-34J helicopters are assumed to be modified in the following manner.

a) Readily removable items not needed in the Heli-Stat application have been removed. These include such items as the landing gear (the Heli-Stat landing gear is mounted on the interconnecting structure), electronics, door, soundproofing, stabilizer and tail pylon.

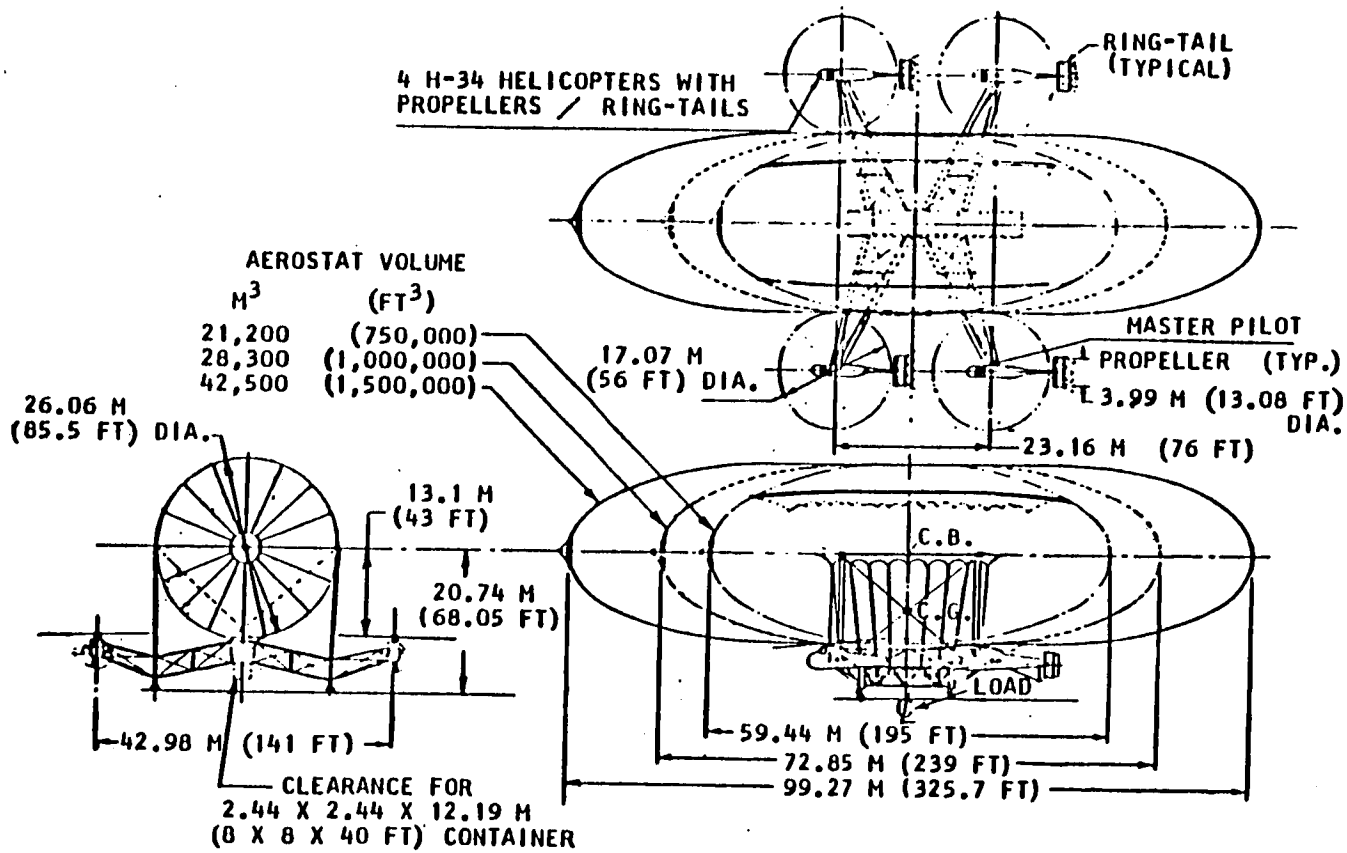

FIG. 1 MATRIX OF DESIGNS FOR STUDY OF HYBRID LTA CONTROLLABILITY

TABLE 1 MATRIX OF HELI-STAT CONFIGURATIONS ANALYZED

AEROSTAT VOLUME m^3 (ft^3)	INFLATION %	BUOYANCY kN (lb (f))	LOAD STATUS -	BUOYANCY RATIO -
21,200 (750,000)	86.2	179.88 (40,470)	Minimum Flying Wt.	0.77
			50% Useful Load	0.56
			Maximum	0.44
	95.0	198.24 (44,601)	Minimum Flying Wt.	0.84
			50% Useful Load	0.60
			Maximum	0.46
28,300 (1,000,000)	86.2	239.84 (53,960)	Minimum Flying Wt.	0.97
			50% Useful Load	0.67
			Maximum	0.51
	95.0	264.33 (59,470)	Minimum Flying Wt.	1.06
			Neutral Buoyancy	1.00
			50% Useful Load	0.71
			Maximum	0.53
42,500 (1,500,000)	86.2	359.76 (80,940)	Minimum Flying Wt.	1.26
			Neutral Buoyancy	1.00
			50% Useful Load	0.82
			Maximum	0.61
	95.0	396.49 (89,203)	Minimum Flying Wt.	1.39
			Neutral Buoyancy	1.00
			50% Useful Load	0.87
			Maximum	0.63

5.1 DESCRIPTION OF HELI-STAT VERSIONS (Cont'd)

b) The helicopter anti-torque rotors are removed from all four helicopters and replaced by airplane-type reversible-pitch propellers. They are not needed, since rotor torque on the Heli-Stat is reacted by differential thrust vectoring of the main rotors. This is an average value which is nearly correct throughout the rotor thrust/power range considered, and is assumed to be rigged in, with the other thrust-vectoring controls operating symmetrically about this point.

Since rotor torque is approximately proportional to rotor thrust, this average value is considered to react the torque with sufficient accuracy throughout the thrust range of the SH-34J rotor, and is treated as a fixed built-in angle with maneuvering control deflections taken equally plus and minus about it. The propellers are capable of providing fore-and-aft thrust, either simultaneous for vectoring in the longitudinal direction, or differentially to produce yaw moments.

c) The propellers mentioned above are mounted in propeller ducts behind which are deflectable vanes capable of vectoring the propeller thrust left or right, called Piasecki Ring-Tails. The lateral thrust components thus produced can act in unison to develop lateral control forces on the Heli-Stat, or differentially to produce yawing moments, both of which are additive to the vectored thrust of the main rotors.

5.1.1 Heli-Stat Control Forces

The control forces about all axes are produced at and by the four helicopters. The main (lifting) rotors can be controlled in collective pitch to vary the magnitude of the rotor thrust, and in cyclic pitch to vector the thrust, both longitudinally and laterally, in the same manner as in the normal SH-34J helicopter. Although the rotor of an SH-34J helicopter does not normally produce negative (downward) thrust as a steady-state condition, for this study it has been assumed that negative thrust is available as required to permit operation in a condition where buoyancy ratio is greater than unity.

TABLE 2. CONSTANT PARAMETERS FOR ALL HELI-STAT VERSIONS IN MATRIX

PARAMETER	UNITS	VALUES
Altitude	——	Sea Level
Temperature	C (F)	15 (59)
Air Density	kg/m^3 (sl/ft^3)	1.225 (.002377)
Longitudinal Rotor Spacing (X_{Rtr})	m (ft)	23.2 (76.)
Lateral Rotor Spacing (Y_{Rtr})	m (ft)	43.0 (141.)
Distance of Rotors Below Center of Buoyancy (H_{Rtr})	m (ft)	13.1 (43.)
Maximum Vectoring Angle of Main Rotor Thrust in X Direction (γ_{Xmax})	deg	12.
in Y Direction (γ_{Ymax})	deg	12.
Main Rotor Maximum Differential Thrust (Each) (ΔTz)	kN (lb f)	13.3 (3,000.)
Main Rotor Differential Thrust Mixing Ratio $K_{\Delta T_Z} = \Delta T_{Zmax} / \gamma_{Ymax}$ = 3,000 lb.(f) ÷ 12 Deg.	kN/deg (lb f/deg)	1.11 (250.)

TABLE 3 HELI-STAT DIMENSIONAL, MASS, AND INERTIAL PROPERTIES

Item	Units	Varying Operational Weights		
Aerostat Volume	m^3 (ft^3)	21,200. (750,000.)		
Helium Inflation	%	86.2		
Load Status		Minimum Flying Wt.	50% Useful Load	Maximum Load
Weight Empty	kg (lb.(m))	23,212 (51,174)	23,212 (51,174)	23,212 (51,174)
Useful Load	kg (lb.(m))	692 (1,526)	9,712 (21,411)	18,732 (41,296)
Gross Weight	kg (lb.(m))	23,904 (52,700)	32,924 (72,585)	41,944 (92,470)
Mass, Including Internal Gases	kg (lb.(m))	31,546 (69,546)	40,565 (89,431)	49,585 (109,316)
Add'l Apparent Mass (Longitudinal Motion) Δm_x	kg (lb.(m))	4,427 (9,759)	4,427 (9,759)	4,427 (9,759)
(Lateral Motion) Δm_y	kg (lb.(m))	18,754 (41,345)	18,754 (41,345)	18,754 (41,345)
Dist. Center of Mass Below Center of Buoy. (H_{cg})	m (ft)	9.34 (30.63)	11.46 (37.61)	12.82 (42.05)
Mass Moment of Inertia About Center of Mass, Including Gases, I_x	$kg \cdot m^2$ ($sl \cdot ft^2$)	10,346,117 (7,630,904)	12,055,284 (8,891,521)	13,525,582 (9,975,957)
I_z	$kg \cdot m^2$ ($sl \cdot ft^2$)	13,120,151 (9,676,927)	14,582,832 (10,755,745)	16,045,850 (11,834,812)
Add'l Apparent Moment of Inertia in Yaw ΔI_z	$kg \cdot m^2$ ($sl \cdot ft^2$)	1,756,191 (1,295,300)	1,756,191 (1,295,300)	1,756,191 (1,295,300)
Max. Propeller Thrust (Each) in X or Y Directions $T_{P_{Xmax}}$ or $T_{P_{Ymax}}$	kN (lb (f))	±15.42 (±3,467)	±10.28 (±2,311)	±5.14 (±1,156)
Propeller Thrust Mixing Ratio (Each Helicopter) $K_{T_{P_X}} = T_{P_X}/\delta_X$	N/deg. (lb(f)/deg)	1,285 (288.9)	856.7 (192.6)	428.5 (96.33)
$K_{T_{P_Y}} = T_{P_Y}/\delta_Y$	N/deg (lb(f)/deg)	1,285 (288.9)	856.7 (192.6)	428.5 (96.33)

TABLE 3 HELI-STAT DIMENSIONAL, MASS, AND INERTIAL PROPERTIES (Cont'd)

Item	Units	Varying Operational Weights		
Aerostat Volume	m^3 (ft^3)	21,200. (750,000.)		
Helium Inflation	%	95.0		
Load Status		Minimum Flying Wt.	50% Useful Load	Maximum Load
Weight Empty	kg (lb.(m))	23,212 (51,174)	23,212 (51,174)	23,212 (51,174)
Useful Load	kg (lb.(m))	692 (1,526)	10,649 (23,476)	20,605 (45,427)
Gross Weight	kg (lb.(m))	23,904 (52,700)	33,861 (74,650)	43,817 (96,601)
Mass, Including Internal Gases	kg (lb.(m))	29,672 (65,415)	39,642 (87,395)	49,585 (109,316)
Add'l Apparent Mass (Longitudinal Motion) Δm_x	kg (lb.(m))	4,427 (9,759)	4,427 (9,759)	4,427 (9,759)
(Lateral Motion) Δm_y	kg (lb.(m))	18,754 (41,345)	18,754 (41,345)	18,754 (41,345)
Dist. Center of Mass Below Center of Buoy. (H_{cg})	m (ft)	9.60 (31.49)	11.96 (39.23)	13.37 (43.86)
Mass Moment of Inertia About Center of Mass, Including Gases, I_X	$kg \cdot m^2$ ($sl \cdot ft^2$)	10,188,899 (7,514,946)	11,912,706 (8,786,361)	13,373,601 (9,863,862)
I_Z	$kg \cdot m^2$ ($sl \cdot ft^2$)	12,893,838 (9,510,007)	14,374,288 (10,601,931)	15,854,718 (11,693,840)
Add'l Apparent Moment of Inertia in Yaw ΔI_Z	$kg \cdot m^2$ ($sl \cdot ft^2$)	1,756,191 (1,295,300)	1,756,191 (1,295,300)	1,756,191 (1,295,300)
Max. Propeller Thrust (Each) in X or Y Directions $T_{P_{Xmax}}$ or $T_{P_{Ymax}}$	kN (lb (f))	±15.42 (±3,467)	±10.28 (±2,311)	±5.14 (±1,156)
Propeller Thrust Mixing Ratio (Each Helicopter) $K_{T_{P_X}} = T_{P_X}/\gamma_X$	N/deg. (lb(f)/deg)	1,285 (288.9)	856.7 (192.6)	428.5 (96.33)
$K_{T_{P_Y}} = T_{P_Y}/\gamma_Y$	N/deg (lb(f)/deg)	1,285 (288.9)	856.7 (192.6)	428.5 (96.33)

TABLE 3 HELI-STAT DIMENSIONAL, MASS, AND INERTIAL PROPERTIES (Cont'd)

Item	Units	Varying Operational Weights		
Aerostat Volume	m^3 (ft^3)	28,300. (1,000,000.)		
Helium Inflation	%	86.2		
Load Status		Minimum Flying Wt.	50% Useful Load	Maximum Load
Weight Empty	kg (lb.(m))	24,895 (54,885)	24,895 (54,885)	24,895 (54,885)
Useful Load	kg (lb.(m))	692 (1,526)	11,930 (26,301)	23,168 (51,076)
Gross Weight	kg (lb.(m))	25,587 (56,411)	36,825 (81,186)	48,063 (105,961)
Mass, Including Internal Gases	kg (lb.(m))	35,792 (78,907)	47,029 (103,682)	58,267 (128,457)
Add'l Apparent Mass (Longitudinal Motion) Δm_x	kg (lb.(m))	4,513 (9,950)	4,513 (9,950)	4,513 (9,950)
(Lateral Motion) Δm_y	kg (lb.(m))	27,430 (60,472)	27,430 (60,472)	27,430 (60,472)
Dist. Center of Mass Below Center of Buoy. (H_{cg})	m (ft)	8.68 (28.48)	11.16 (36.63)	12.69 (41.64)
Mass Moment of Inertia About Center of Mass, Including Gases, I_x	$kg \cdot m^2$ ($sl \cdot ft^2$)	12,954,499 (9,554,748)	14,981,018 (11,049,432)	16,587,897 (12,234,605)
I_z	$kg \cdot m^2$ ($sl \cdot ft^2$)	15,821,510 (11,669,347)	17,406,490 (12,838,368)	18,988,827 (14,005,440)
Add'l Apparent Moment of Inertia in Yaw ΔI_z	$kg \cdot m^2$ ($sl \cdot ft^2$)	4,854,518 (3,580,509)	4,854,518 (3,580,509)	4,854,518 (3,580,509)
Max. Propeller Thrust (Each) in X or Y Directions $T_{P_{Xmax}}$ or $T_{P_{Ymax}}$	kN (lb (f))	±15.42 (±3,467)	±10.28 (±2,311)	±5.14 (±1,156)
Propeller Thrust Mixing Ratio (Each Helicopter) $K_{T_{P_X}} = T_{P_X}/\gamma_X$	N/deg. (lb(f)/deg)	1,285 (288.9)	856.7 (192.6)	428.5 (96.33)
$K_{T_{P_Y}} = T_{P_Y}/\gamma_Y$	N/deg (lb(f)/deg)	1,285 (288.9)	856.7 (192.6)	428.5 (96.33)

TABLE 3 HELI-STAT DIMENSIONAL, MASS, AND INERTIAL PROPERTIES (Cont'd)

Item	Units	Varying Operational Weights		
Aerostat Volume	m^3 (ft^3)	28,300. (1,000,000.)		
Helium Inflation	%	95.0		
Load Status		Minimum Flying Wt.	50% Useful Load	Maximum Load
Weight Empty	kg (lb.(m))	24,895 (54,885)	24,895 (54,885)	24,895 (54,885)
Useful Load	kg (lb.(m))	692 (1,526)	13,179 (29,055)	25,667 (56,585)
Gross Weight	kg (lb.(m))	25,587 (56,411)	38,074 (83,940)	50,562 (111,470)
Mass, Including Internal Gases	kg (lb.(m))	33,293 (73,398)	45,780 (100,927)	58,267 (128,457)
Add'l Apparent Mass (Longitudinal Motion) Δm_x	kg (lb.(m))	4,513 (9,950)	4,513 (9,950)	4,513 (9,950)
(Lateral Motion) — Δm_y	kg (lb.(m))	27,430 (60,472)	27,430 (60,472)	27,430 (60,472)
Dist. Center of Mass Below Center of Buoy. (H_{cg})	m (ft)	8.94 (29.34)	11.73 (38.48)	13.32 (43.70)
Mass Moment of Inertia About Center of Mass, Including Gases, I_x	$kg \cdot m^2$ ($sl \cdot ft^2$)	12,721,320 (9,382,764)	14,738,214 (10,870,349)	16,350,378 (12,059,420)
I_z	$kg \cdot m^2$ ($sl \cdot ft^2$)	15,396,396 (11,355,799)	17,014,051 (12,548,920)	18,630,650 (13,741,262)
Add'l Apparent Moment of Inertia in Yaw ΔI_z	$kg \cdot m^2$ ($sl \cdot ft^2$)	4,854,518 (3,580,509)	4,854,518 (3,580,509)	4,854,518 (3,580,509)
Max. Propeller Thrust (Each) in X or Y Directions $T_{P_{Xmax}}$ or $T_{P_{Ymax}}$	kN (lb (f))	±15.42 (±3,467)	±10.28 (±2,311)	±5.14 (±1,156)
Propeller Thrust Mixing Ratio (Each Helicopter) $K_{T_{P_X}} = T_{P_X}/\gamma_X$	N/deg. (lb(f)/deg)	-1,285 (-288.9)	856.7 (192.6)	428.5 (96.33)
$K_{T_{P_Y}} = T_{P_Y}/\gamma_Y$	N/deg (lb(f)/deg)	-1,285 (-288.9)	856.7 (192.6)	428.5 (96.33)

TABLE 3 HELI-STAT DIMENSIONAL, MASS, AND INERTIAL PROPERTIES (Cont'd)

Item	Units	Varying Operational Weights		
Aerostat Volume	m^3 (ft^3)	42,500. (1,500,000.)		
Helium Inflation	%	86.2		
Load Status		Minimum Flying Wt.	50% Useful Load	Maximum Load
Weight Empty	kg (lb.(m))	28,487 (62,804)	28,487 (62,804)	28,487 (62,804)
Useful Load	kg (lb.(m))	692 (1,526)	16,253 (35,831)	31,813 (70,136)
Gross Weight	kg (lb.(m))	29,179 (64,330)	44,740 (98,635)	60,300 (132,940)
Mass, Including Internal Gases	kg (lb.(m))	44,462 (98,022)	60,023 (132,327)	75,583 (166,632)
Add'l Apparent Mass (Longitudinal Motion) Δm_x	kg (lb.(m))	4,513 (9,950)	4,513 (9,950)	4,513 (9,950)
(Lateral Motion) Δm_y	kg (lb.(m))	44,270 (97,598)	44,270 (97,598)	44,270 (97,598)
Dist. Center of Mass Below Center of Buoy. (H_{cg})	m (ft)	7.74 (25.38)	10.73 (35.20)	12.49 (40.98)
Mass Moment of Inertia About Center of Mass, Including Gases, I_x	$kg \cdot m^2$ ($sl \cdot ft^2$)	12,331,658 (9,095,364)	14,943,844 (11,022,014)	16,923,081 (12,481,824)
I_z	$kg \cdot m^2$ ($sl \cdot ft^2$)	24,941,661 (18,396,025)	26,781,095 (19,752,722)	28,620,050 (21,109,066)
Add'l Apparent Moment of Inertia in Yaw ΔI_z	$kg \cdot m^2$ ($sl \cdot ft^2$)	18,738,946 (13,821,137)	18,738,946 (13,821,137)	18,738,946 (13,821,137)
Max. Propeller Thrust (Each) in X or Y Directions $T_{P_{Xmax}}$ or $T_{P_{Ymax}}$	kN (lb (f))	±10.14 (±2,280)	±10.28 (±2,311)	±5.14 (±1,156)
Propeller Thrust Mixing Ratio (Each Helicopter) $K_{T_{P_X}} = T_{P_X}/\gamma_X$	N/deg. (lb(f)/deg)	-845. (-190.)	856.7 (192.6)	428.5 (96.33)
$K_{T_{P_Y}} = T_{P_Y}/\gamma_Y$	N/deg (lb(f)/deg)	-845. (-190.)	856.7 (192.6)	428.5 (96.33)

TABLE 3 HELI-STAT DIMENSIONAL, MASS, AND INERTIAL PROPERTIES (Cont'd)

Item	Units	Varying Operational Weights		
Aerostat Volume	m^3 (ft^3)	42,500. (1,500,000.)		
Helium Inflation	%	95.0		
Load Status		Minimum Flying Wt.	50% Useful Load	Maximum Load
Weight Empty	kg (lb.(m))	28,487 (62,804)	28,487 (62,804)	28,487 (62,804)
Useful Load	kg (lb.(m))	692 (1,526)	18,126 (39,962)	35,561 (78,399)
Gross Weight	kg (lb.(m))	29,179 (64,330)	46,613 (102,766)	64,048 (141,203)
Mass, Including Internal Gases	kg (lb.(m))	40,714 (89,759)	58,148 (128,195)	75,583 (166,632)
Add'l Apparent Mass (Longitudinal Motion) Δm_x	kg (lb.(m))	4,513 (9,950)	4,513 (9,950)	4,513 (9,950)
(Lateral Motion) Δm_y	kg (lb.(m))	44,270 (97,598)	44,270 (97,598)	44,270 (97,598)
Dist. Center of Mass Below Center of Buoy. (H_{cg})	m (ft)	7.97 (26.15)	11.38 (37.34)	13.22 (43.36)
Mass Moment of Inertia About Center of Mass, Including Gases, I_X	$kg \cdot m^2$ ($sl \cdot ft^2$)	12,004,689 (8,854,204)	14,659,771 (10,812,492)	16,590,255 (12,236,344)
I_Z	$kg \cdot m^2$ ($sl \cdot ft^2$)	23,800,759 (17,554,539)	25,711,684 (18,963,965)	27,621,747 (20,372,755)
Add'l Apparent Moment of Inertia in Yaw ΔI_Z	$kg \cdot m^2$ ($sl \cdot ft^2$)	18,738,946 (13,821,137)	18,738,946 (13,821,137)	18,738,946 (13,821,137)
Max. Propeller Thrust (Each) in X or Y Directions $T_{P_{Xmax}}$ or $T_{P_{Ymax}}$	kN (lb (f))	±9.61 (±2,160)	±10.28 (±2,311)	±5.14 (±1,156)
Propeller Thrust Mixing Ratio (Each Helicopter) $K_{T_{P_X}} = T_{P_X}/\gamma_X$	N/deg. (lb(f)/deg)	-801. (-180.)	856.7 (192.6)	428.5 (96.33)
$K_{T_{P_Y}} = T_{P_Y}/\gamma_Y$	N/deg (lb(f)/deg)	-801. (-180.)	856.7 (192.6)	428.5 (96.33)

TABLE 3 HELI-STAT DIMENSIONAL, MASS, AND INERTIAL PROPERTIES (Cont'd)

Item	Units	Varying Operational Weights	
Aerostat Volume	m^3 (ft^3)	28,300 (1,000,000.)	42,500 (1,500,000.)
Helium Inflation	%	95.0	86.2
Load Status		Neutral Buoyancy	Neutral Buoyancy
Weight Empty	kg (lb.(m))	24,895 (54,885)	28,487 (62,804)
Useful Load	kg (lb.(m))	2,117 (4,667)	8,307 (18,313)
Gross Weight	kg (lb.(m))	27,012 (59,552)	36,794 (81,117)
Mass, Including Internal Gases	kg (lb.(m))	34,718 (76,539)	52,076 (114,809)
Add'l Apparent Mass (Longitudinal Motion) Δm_x	kg (lb.(m))	4,513 (9,950)	4,513 (9,950)
(Lateral Motion) Δm_y	kg (lb.(m))	27,430 (60,472)	44,270 (97,598)
Dist. Center of Mass Below Center of Buoy. (H_{cg})	m (ft)	8.23 (27.0)	8.83 (28.98)
Mass Moment of Inertia About Center of Mass, Including Gases, I_x	$kg \cdot m^2$ ($sl \cdot ft^2$)	12,200,000 (9,000,000)	13,600,000 (10,000,000)
I_z	$kg \cdot m^2$ ($sl \cdot ft^2$)	14,900,000 (11,000,000)	25,800,000 (19,000,000)
Add'l Apparent Moment of Inertia in Yaw ΔI_z	$kg \cdot m^2$ ($sl \cdot ft^2$)	4,854,518 (3,580,509)	18,738,946 (13,821,137)
Max. Propeller Thrust (Each) in X or Y Directions (Each) $T_{P_{Xmax}}$ or $T_{P_{Ymax}}$	kN (lb (f))	±15.42 (±3,467)	±15.42 (±3,467)
Propeller Thrust Mixing Ratio (Each Helicopter) $K_{T_{P_X}} = T_{P_X}/\gamma_X$	N/deg. (lb(f)/deg)	1,285. (288.9)	1,285. (288.9)
$K_{T_{P_Y}} = T_{P_Y}/\gamma_Y$	N/deg (lb(f)/deg)	1,285. (288.9)	1,285. (288.9)

TABLE 4 AERODYNAMIC FORCES AND MOMENTS ON HELI-STAT

ITEM	UNITS	VALUES		
Aerostat Volume	m^3 (ft^3)	21,200 (750,000)		
Overall Length	m (ft)	59.4 (195.)		
Maximum Diameter	m (ft)	26.1 (85.5)		
Fineness Ratio (L/D)	—	2.28		
Yawing Inertia Co-efficient $K_2 - K_1$ (Ref.4, Fig.1, Pg.4)	—	0.55		
Load Status	—	Minimum Flying Wt.	50% Useful Load	Maximum Load
Sideslip Angle	deg	0	0	0
Equivalent Drag Area	m^2 (ft^2)	60.8 (654.)	63.7 (686.)	63.7 (686.)
Sideslip Angle	deg	20	20	20
Equivalent Drag Area	m^2 (ft^2)	100.1 (1077.)	101.1 (1088.)	105.4 (1135.)
Sideslip Angle	deg	40	40	40
Equivalent Drag Area	m^2 (ft^2)	199.6 (2148.)	203.3 (2188.)	211.1 (2272.)
Sideslip Angle	deg	60	60	60
Equivalent Drag Area	m^2 (ft^2)	312.6 (3365.)	319.4 (3438.)	331.2 (3565.)
Sideslip Angle	deg	90	90	90
Equivalent Drag Area	m^2 (ft^2)	396.6 (4269.)	408.5 (4397.)	420.4 (4525.)

TABLE 4 AERODYNAMIC FORCES AND MOMENTS ON HELI-STAT (Cont'd)

ITEM	UNITS	VALUES		
Aerostat Volume	m^3 (ft^3)	28,300 (1,000,000)		
Overall Length	m (ft)	72.8 (239.)		
Maximum Diameter	m (ft)	26.1 (85.5)		
Fineness Ratio (L/D)	—	2.79		
Yawing Inertia Co-efficient $K_2 - K_1$ (Ref.4, Fig.1, Pg.4)	—	0.66		
Load Status	—	Minimum Flying Wt.	50% Useful Load	Maximum Load
Sideslip Angle	deg	0	0	0
Equivalent Drag Area	m^2 (ft^2)	60.8 (654.)	63.7 (686.)	63.7 (686.)
Sideslip Angle	deg	20	20	20
Equivalent Drag Area	m^2 (ft^2)	115.9 (1247.)	119.8 (1290.)	121.2 (1305.)
Sideslip Angle	deg	40	40	40
Equivalent Drag Area	m^2 (ft^2)	255.3 (2748.)	261.9 (2819.)	266.8 (2872.)
Sideslip Angle	deg	60	60	60
Equivalent Drag Area	m^2 (ft^2)	413.8 (4454.)	423.5 (4558.)	432.4 (4654.)
Sideslip Angle	deg	90	90	90
Equivalent Drag Area	m^2 (ft^2)	531.5 (5721.)	543.4 (5849.)	555.3 (5977.)

TABLE 4 AERODYNAMIC FORCES AND MOMENTS ON HELI-STAT (Cont'd)

ITEM	UNITS	VALUES		
Aerostat Volume	m^3 (ft^3)	42,500 (1,500,000)		
Overall Length	m (ft)	99.3 (325.7)		
Maximum Diameter	m (ft)	26.1 (85.5)		
Fineness Ratio (L/D)	—	3.80		
Yawing Inertia Co-efficient $K_2 - K_1$ (Ref.4, Fig.1, Pg.4)	—	0.77		
Load Status	—	Minimum Flying Wt.	Neutral Buoyancy	Maximum Load
Sideslip Angle	deg	0	0	0
Equivalent Drag Area	m^2 (ft^2)	63.4 (682.)	64.1 (690.)	66.3 (714.)
Sideslip Angle	deg	20	20	20
Equivalent Drag Area	m^2 (ft^2)	149.7 (1611)	150.5 (1620)	155.1 (1670)
Sideslip Angle	deg	40	40	40
Equivalent Drag Area	m^2 (ft^2)	368.2 (3964)	370.7 (3990)	379.9 (4089)
Sideslip Angle	deg	60	60	60
Equivalent Drag Area	m^2 (ft^2)	616.9 (6640)	622.5 (6700)	635.5 (6840)
Sideslip Angle	deg	90	90	90
Equivalent Drag Area	m^2 (ft^2)	801.4 (8626)	807.3 (8690)	825.2 (8882)

All four rotors can be vectored in unison foreward or aft to produce accelerating forces along the X-axis, or left or right for the Y-axis. They can also be vectored differentially in both axes to produce yaw moments about the Z-axis. Thus, to produce a yawing moment to the right the two forward rotors are vectored to the right, the two aft rotors are vectored to the left, the two starboard rotors are vectored aft, and the two port rotors are vectored forward.

Cyclic pitch range is assumed to be $\pm$ 12 degrees in both axes, typical of helicopter rotors, and includes yaw control combined with longitudinal or/and lateral control.

In order to produce roll moments on the Heli-Stat the helicopter rotors are controlled differentially in collective pitch to produce differential thrust on the left and right pairs. The maximum differential thrust available is assumed to be $\pm$ 13.3 kN ($\pm$ 3,000 pounds force), which is a typical value for the differential thrust for a twin rotor helicopter with rotors of comparable thrust rating.

Rotor torque on a normal, separately operating SH-34J helicopter is reacted by a couple produced by an anti-torque tail rotor and a lateral component of the main rotor. The rotors of the Heli-Stat are so widely spaced, however, that their torques are easily reacted by small horizontal thrust components at each rotor, produced by differential longitudinal vectoring of about $\pm$ 4 degrees.

Since the SH-34J tail rotors are not needed for anti-torque, they are considered to be removed and are replaced by Piasecki Ring-Tails, which are fore-and-aft thrusting propellers mounted in ducts behind which are deflecting vanes which can vector the propeller thrust left or right. These vectored propeller thrusts (fore-and-aft, left and right, and either simultaneous or differential) are used in conjunction with and additive to the vectored main-rotor thrusts. The propellers are driven from the helicopters' drive system with power from the same engine which drives the main rotor. Thus with maximum gross weight loading of the Heli-Stat, most of the available power is directed to the main rotors, with secondary control forces provided by the Ring-Tails (or propellers).

With lightly loaded rotors, however, as in nearly neutral buoyancy, the main rotors produce little thrust, consume little power, but contribute to controllability, and allow most of the power to be diverted to the Ring-Tails which then become the prime sources of control and propulsion forces.

Main rotor power at the various thrust levels used in the analysis was calculated from flight test data on the H-34 helicopter (Ref. 5). The balance of the available power from each helicopter is then assumed to be available to its Ring-Tail for maximum control thrust, which was calculated from performance data supplied by Hamilton Standard Div. of United Technologies.

The Ring-Tail thrust values included a correction for 15% loss at the angles of turn used and for the sine of the angle of deflection. For simplicity these same values were used for $\pm T_{P_X\ max}$, and it was assumed that the X and Y components of propeller thrust were attainable simultaneously when required.

With so many degrees of freedom in the controls there would be an infinite set of combinations which could be used to trim the Heli-Stat. To make the analysis tractable, yet consistent with a potential real design, the controls are assumed to be co-ordinated by mixing linkages as follows.

1. The control parameter in terms of which the others are related is taken as γ, the vectoring angle of the main rotor thrust, with subscript x or y to denote the direction of vectoring. It is not to be implied that γ is the most powerful or most important control. It is merely a convenient parameter with respect to which mixing ratios can be established for the others.

2. For a given configuration there is a fixed linear relation between γ_X and T_{P_X}, the Ring-Tail (or propeller) thrust in the X direction, and between γ_Y and T_{P_Y}; also between γ_Y and ΔT_Z, the main-rotor differential thrust for roll control.

3. The linear relationships are such that $\gamma_{Y\ max}$ (12 degrees) corresponds with $\Delta T_{Z\ max}$ (3,000 pounds), and with $T_{P_{Y}\ max}$; also $\gamma_{X\ max}$ (12 degrees) corresponds with $T_{P_{X}\ max}$. $T_{P_{X}\ max}$ and $T_{P_{Y}\ max}$ are determined by the power available to the propeller at the particular loading condition, and it is assumed that the propeller controls are adjustable to provide this feature. The 12-degree figure for $\gamma_{X\ max}$ corresponds to the control limits on the SH-34J helicopter. Thus the mixing ratios were chosen to use all the control available from the SH-34J, and all the excess power available to the propellers.

4. For yaw control, involving $\Delta T_{P_{X}}$, $\Delta T_{P_{Y}}$, $\Delta\gamma_{X}$ and $\Delta\gamma_{Y}$, it is assumed that $\Delta T_{P_{X}} = \Delta T_{P_{Y}}$, and $\Delta\gamma_{X} = \Delta\gamma_{Y}$.

5. Whenever the buoyancy ratio is greater than one (negative rotor thrust) the ratios of $T_{P_{X}}$ to γ_{X} and $T_{P_{Y}}$ to γ_{Y} are reversed in sign because of the reversal in sign of the main-rotor thrust. It is assumed that means are provided in the control system to accomplish this.

Lighter-than-air ships conventionally use their ballonets for attitude trim by pumping air from one ballonet to another. For airships which lack dynamic thrusters, this is a trimming means available at low airspeed where tail surfaces are relatively ineffective. However, transfer of a large mass of air is a slow process. Although the Heli-Stat has ballonets, which could be used for trimming, their primary function is to maintain constant volume under varying external pressure. Differential rotor collective pitch affords a more rapid means of trimming.

5.2 ANALYTICAL PROCEDURE

The general method employed in the analysis involved the following steps.

a) The mass, center-of-gravity locations, and moments of inertia were calculated of each individual version for each loading condition. The "free body" which is acted upon by external forces is the complete vehicle and includes all internal gases (helium in the main envelope and air in the ballonets for the particular inflation condition considered). The mass, center-of-gravity, and moments of inertia were calculated for this overall mass. Payload was considered to consist of one or more international standard containers, 2.44 x 2.44 x 12.19 m (8 x 8 x 40 ft.), attached immediately under the center keel structure (Figure 1). A summary of mass and inertial properties of all versions is given in Table 3.

b) The effective drag area of each version was estimated for sideslip angles of zero and 90 degrees. The zero-degree drag coefficients (based on frontal area) for the buoyant envelopes are taken from Figure 19, page 3-12 of Ref. 2, for turbulent flow on ellipsoidal bodies. These values are conservative because the Reynolds number in the reference figure (based on overall length), although in the turbulent flow regime, is nevertheless only 10^6. The Reynolds number of these vehicles would be of the order of 5×10^7 at a speed of 20 knots. This higher Reynolds number should result in a significantly lower drag coefficient, although actual data on ellipsoidal shapes at such large Reynolds numbers is not available. For the 90-degree sideslip the shapes of the envelope, which actually consist of a cylindrical midsection with ellipsoidal ends, were approximated by a cylindrical midsection with hemispherical ends and the same overall volume. Figure 12, page 3-9 of Ref. 2 was used for the cylindrical portion, and Figure 19, page 3-12 of the same reference was used for the hemispherical ends.

The equivalent drag area of the helicopters, alone, at zero degrees was derived from flight test data on the SH-34A helicopter (Ref. 5).

The equivalent drag area for the interconnecting structure was calculated by conventional airplane-technology methods using appropriate data from Ref. 2 as follows. A drag coefficient of 0.5 for the longitudinal keel (at zero sideslip)

was obtained from Figure 22, page 3-12. For the landing wheels 0.15 was taken from Figure 33, page 13-14. Struts and wires were assumed to be of streamline shape with chord/thickness ratio of 2.7, and a drag coefficient of 0.055 from Figure 10, page 6-9, was used, corresponding to a friction drag coefficient, c_f, of 0.0038. Corrections for struts and wires in oblique planes were made by means of the "cross flow principle" per page 3-11 (Ref. 2).

For intermediate sideslip angles published data is practically non-existent beyond about 15 degrees. Accordingly, drags for angles between zero and 90° were established by fitting an S-shaped sine-squared curve between those points, according to the expression

$$S_\beta = S_o + (S_{90} - S_o) \sin^2 \beta \qquad (1)$$

which is seen to match the zero and 90-degree points. In this expression, S is the total equivalent drag area, β is a sideslip angle, and subscripts 0, 90, and β refer to the values at 0, 90, and degrees, respectively.

c) Aerodynamic yawing moments at sideslip angles greater than zero were calculated using the expression

$$\text{Yawing moment, } M_Z = \frac{1}{2}\rho V^2 \mp (k_2 - k_1) \sin 2\beta \qquad (2)$$

per equation (7), page 7 of Ref. 4. The inertia coefficients k_1 and k_2 are given in Figure 1, page 4 of that reference (see Section 9 for definitions).

d) At each wind speed (relative airspeed for a nominal hover condition) and sideslip angle, the required values for the control parameters described in Section 5.1.1 were calculated to trim the vehicle simultaneously for sideslip speed component, roll, longitudinal speed component, and yawing moment. The maximum control remaining in each axis (considered separately) was then applied and the resulting acceleration calculated for each axis.

e) Maximum accelerations (each axis) versus windspeed for given sideslip angles were plotted, and are shown in Section 6, Results. The points of zero acceleration capability determine the limiting windspeed/sideslip combination. Where these values differ for different axes (e.g. roll vs. yaw), the lower speed governs, since at any higher speed the vehicle cannot be trimmed in all axes without running out of control in some axis.

In the calculation sequence the vehicle was first trimmed for roll and lateral translation. A free-body diagram, with all forces, is shown in Figure 7. The static trim equations are:

$$\Sigma Z = 0 \qquad L_B + 4T_R \cos(\phi + \gamma_Y) - 4T_{P_Y} \sin\phi - W = 0 \tag{3}$$

$$\Sigma Y = 0 \qquad 4\,T_R \sin(\phi + \gamma_Y) + 4T_{P_Y} \cos\phi - D \sin\beta - L_{CW} \cos\beta = 0 \tag{4}$$

$$\Sigma M_{X_{CB}} = 0 \qquad 2\,\Delta T_Z\, Y_{RTR} - L_B\, H_{CG} \sin\phi - 4T_R \sin\gamma_Y\,(H_{RTR} - H_{CG}) - D\, H_{CG} \sin\beta \cos\phi + L_{CW}\, H_{CG} \cos\beta \cos\phi - 4\,T_{P_Y}\,(H_{RTR} - H_{CG}) = 0 \tag{5}$$

Solving equation (3) for T_R and substituting for T_R in equations (4) and (5), in turn, yield equations (6) and (7).

$$\left[4\,T_{P_Y} \sin\phi + (W - L_B)\right] \tan(\phi + \gamma_Y) + 4\,T_{P_Y} \cos\phi - D \sin\beta - L_{CW} \cos\beta = 0 \tag{6}$$

$$2\,\Delta T_Z\, Y_{RTR} - \left(\frac{4T_{P_Y} \sin\phi + (W - L_B)}{\cos(\phi + \gamma_Y)}\right) \sin\gamma_Y\,(H_{RTR} - H_{CG}) - D\, H_{CG} \sin\beta \cos\phi + L_{CW}\, H_{CG} \cos\beta \cos\phi - L_B\, H_{CG} \sin\phi - 4\,T_{P_Y}\,(H_{RTR} - H_{CG}) = 0 \tag{7}$$

No data was available for the C_L of airship shapes at angles of attack above 20 degrees, and no data at all on ellipsoids. In the analyses presented herein the terms involving L_{CW} (and thus C_L) were not used in the calculations. Subsequent review, for the 1,000,000 ft^3 aerostat, using assumed C_L's above 20 degrees, showed that the reduction in maximum trimmable crosswind speed ascribable to this effect is of the order of two knots, and occurs in the vicinity of 40-degree sideslip angle. The difference decreases rapidly above 45 degrees and, of course, becomes zero at 90 degrees.

Induced drag was not separately calculated, it was included in the total drag, computed as described in Section 5.2(b).

The control parameters, T_{P_Y} and ΔT_Z, were eliminated in equations (6) and (7) by substituting their relationships to γ_Y described in Section 5.1.1. After making these substitutions, equations (6) and (7) each have only two unknowns, ϕ and γ_Y. They were each solved for γ_Y by computer trial-and error methods at several arbitrary values of ϕ for each specific configuration (volume, loading condition, air-speed, sideslip angle). Pairs of values of ϕ and γ_Y satisfying equation (6) represent a vehicle trimmed in lateral translation, but not necessarily in roll. Pairs of values satisfying equation (7) represent trim in roll but necessarily in lateral translation. These pairs of values were plotted, one against the other, for a series of constant speeds. The intersections of the resulting graphs yield pairs of ϕ and γ_Y representing conditions trimmed in both roll and lateral translation.

The vehicle was next trimmed for longitudinal translation by equating all X-forces to zero, equation (8).

$$\Sigma X = 0 \qquad 4\, T_R \sin\gamma_X - D\cos\beta + 4\, T_{P_X} + L_{CW}\sin\beta = 0 \qquad (8)$$

Equation (8) was solved for γ_X after substituting for T_{P_X} its equivalent function of γ_X (as described in Section 5.1.1) and for T_R from equation (3).

The vehicle was assumed to maintain its longitudinal axis horizontal, using differential rotor thrust as required. Since the lateral/roll trim calculations showed that differential rotor thrust available for roll was never a limiting factor, and since in the worst case investigated (35 knots with the largest envelope size) only 28% of the differential thrust available was required for pitch trim, this calculation was omitted in the trim procedure.

The vehicle was next trimmed in yaw by equating all yawing moments to zero, equation (9).

$$\Sigma M_Z = 0 \quad 2\, X_{RTR}\, (\Delta T_{P_Y} + \Delta T_{R_Y}) \cos \phi + 2\, Y_{RTR}\, (\Delta T_{P_X} + \Delta T_{R_X}) - M_Z = 0 \qquad (9)$$

The aerodynamic yawing moment, M_Z, is not affected by the term $L_{CW} \cos \beta$, previously mentioned, which is taken to act through the center of buoyancy. M_Z is a pure moment around the center of buoyancy and was calculated independently, from equation (2).

The parameters ΔT_{P_Y}, ΔT_{P_X}, and ΔT_{R_X} were replaced by their respective functions of $\Delta\gamma_X$ and $\Delta\gamma_Y$. (As stated in Section 5.1.1, to reduce the number of independent variables $\Delta\gamma_X = \Delta\gamma_Y$.) With these substitutions equation (9) was then solved for Δ_X and Δ_Y.

The vehicle has been trimmed simultaneously in lateral translation, roll, longitudinal translation, and yaw. Finally, the maximum accelerations were calculated from the amount of control remaining after trimming simultaneously in all of these axes. The mass against which the accelerating forces act includes the additional apparent mass of the surrounding air in the longitudinal and transverse directions, as applicable. Likewise the moment of inertia for yaw acceleration includes the additional apparent moment of inertia. These quantities are given in Table 3, and are derived using the coefficients shown in Figure 1 of Ref. 4.

Calculation of the stability characteristics was beyond the scope of this effort. Stability effects were not considered, except that for each axis accelerations were calculated in the direction of least control remaining from the trim condition. In the yaw axis, therefore, where the body is inherently aerodynamically unstable without tail surfaces (which were assumed not to be incorporated), the analysis does not provide control margin to allow for dynamic overshoot, therefore operational angles will be limited to values lower than calculated herein.

6. RESULTS

6.1 ACCELERATION CAPABILITY IN CROSSWINDS

The acceleration capabilities of the Heli-Stat versions in lateral, longitudinal, and yaw motion while hovering in crosswinds are presented in Figures 2, 3, and 4 respectively. Each axis will be discussed separately.

In some cases the graphs have end-points labeled "maximum trimmable airspeed". Although such a graph appears to retain a significant acceleration capability at these points, the vehicle cannot be trimmed about all axes because the control limit has been reached for one of the other axes. This happens, for example, in longitudinal acceleration at large side-slip angles. Above some critical wind speed there may be insufficient lateral control for trim at that sideslip angle, although the vehicle would otherwise be capable of longitudinal acceleration.

6.1.1 Lateral Acceleration

The three graphs grouped together as Figure 2 show linear acceleration capability in the lateral (Y) direction as a function of wind speed for sideslip angles of 0, 20, 40, 60 and 90 degrees, and for several conditions of loading varying from minimum flying weight to maximum weight as limited by the allowable thrust on the SH-34J rotors, 57.8 kN (13,000 lb.) each. Figure 2(a) shows this capability for the version with a 21,200 m^3 (750,000 ft^3) aerostat. Figure 2(b) shows it for the 28,300 m^3 (1,000,000 ft^3) volume, and Figure 2(c) shows it for the 42,500 m^3 (1,500,000 ft^3) volume.

Referring to Figure 2(a) the decrease in lateral acceleration capability with decreasing buoyancy ratio is clearly evident, especially at very low wind speeds. The reason for this relationship is that the same values of rotor and propeller forces are available to accelerate an inertial mass which increases with decreased buoyancy ratio. The same general relationships are shown in Figures 2(b) and 2(c). Moreover, if these three figures are compared with each other, particularly at near-zero wind speeds, it is seen that the larger the volume of the Heli-Stat, with corresponding larger inertial mass, the

FIG. 2(a) HELI-STAT LATERAL ACCELERATION CAPABILITY IN HOVER VS.WIND SPEED

SEA LEVEL, 15° C (59°F.)

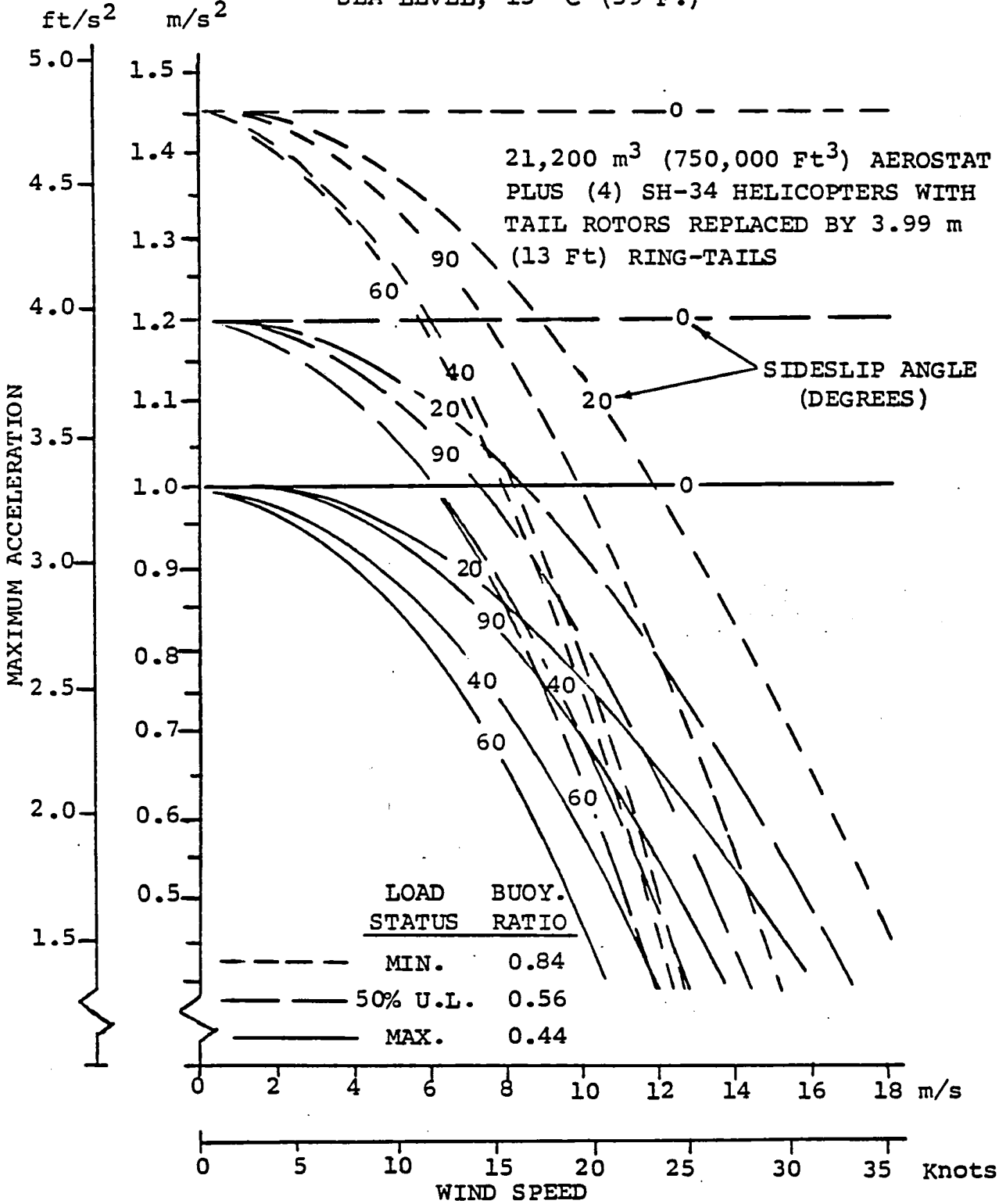

FIG. 2(b) HELI-STAT LATERAL ACCELERATION CAPABILITY IN HOVER VS. WIND SPEED (Cont'd)

SEA LEVEL, 15° C (59°F.)

28,300 m^3 (1,000,000 Ft^3) AEROSTAT PLUS (4) SH-34 HELICOPTERS WITH TAIL ROTORS REPLACED BY 3.99 m (13 Ft) RING-TAILS

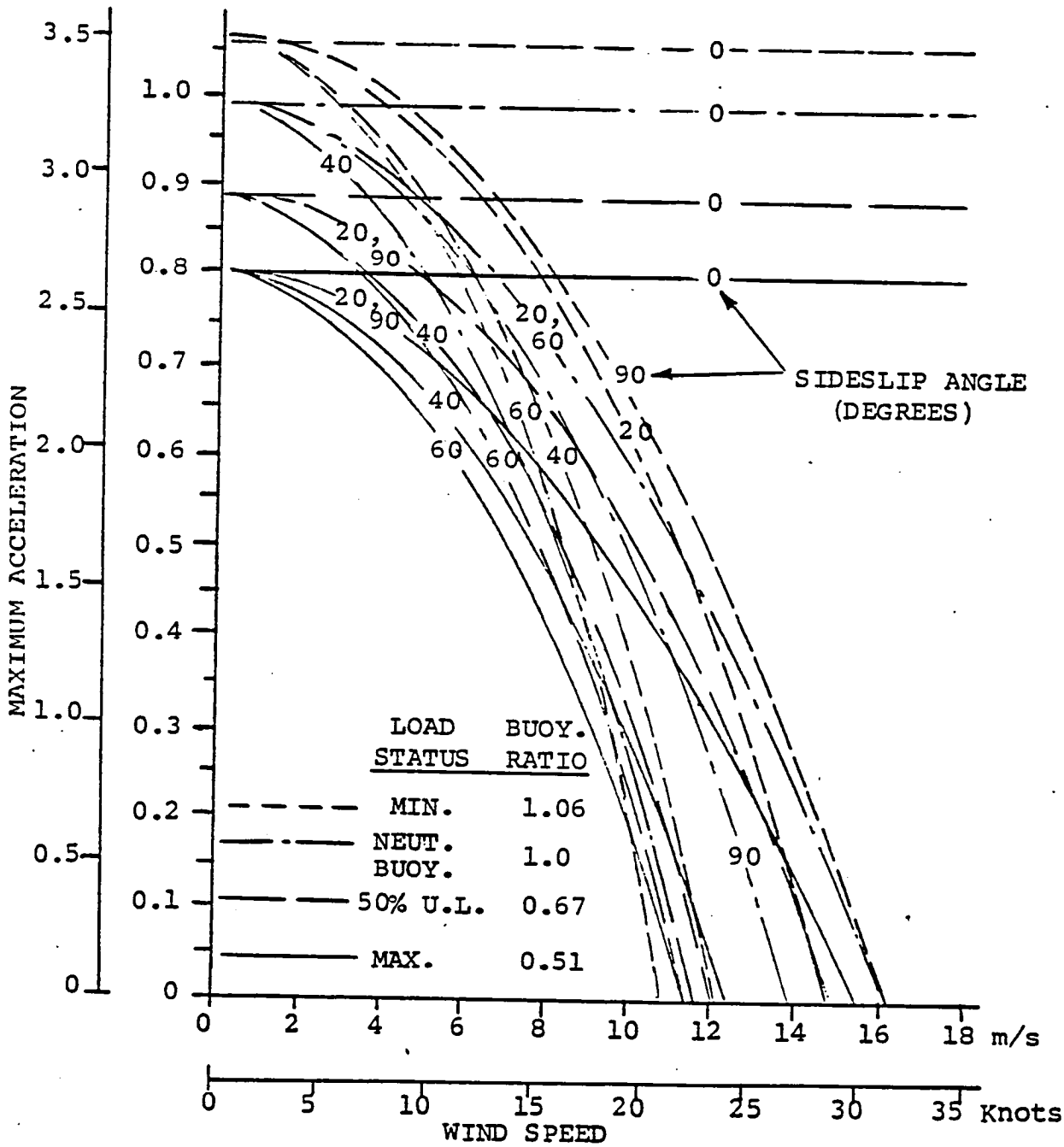

FIG. 2(c) HELI-STAT LATERAL ACCELERATION CAPABILITY IN HOVER VS. WIND SPEED (Cont'd)

SEA LEVEL, 15° C (59°F.)

42,500 m^3 (1,500,000 Ft^3) AEROSTAT PLUS (4) SH-34 HELICOPTERS WITH TAIL ROTORS REPLACED BY 3.99 m (13 Ft) RING-TAILS

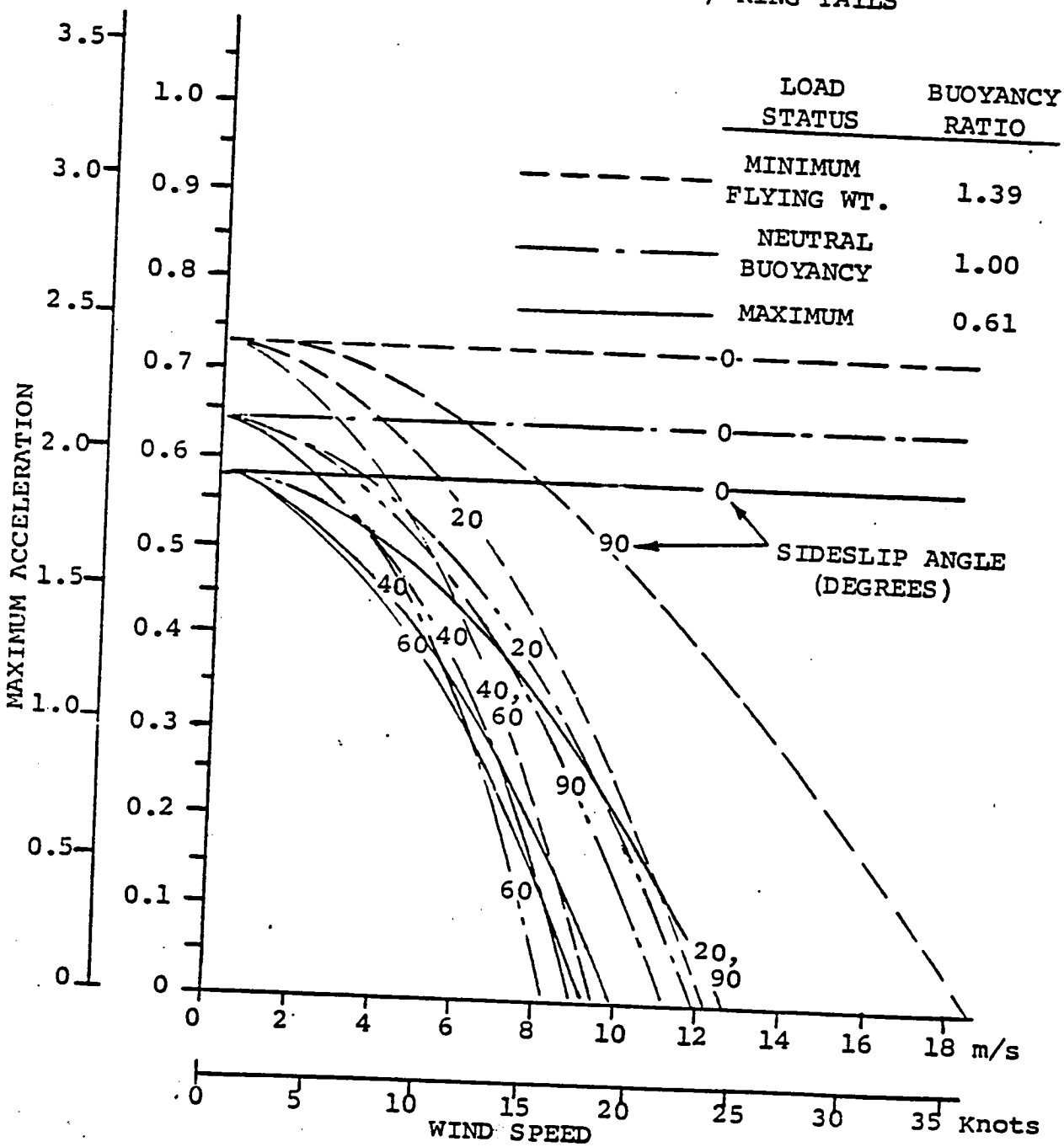

less the acceleration capability. Thus the 21,300 m^3 (750,000 ft^3) version, fully loaded, can accelerate at zero wind speed at 1.0 m/s^2 (3.3 ft/s^2) compared to 0.58 m/s^2 (1.9 ft/s^2) for the 42,500 m^3 (1,500,000 ft^3) version.

Figure 2(c) illustrates another interesting feature, namely that, provided there is an auxiliary lateral thruster independent of the lifting rotors, acceleration capability can be maintained when operating at a buoyancy ratio near unity. In the configurations examined in this study the same powerplant which drives the main rotor of each helicopter also drives the propeller in the Ring-Tail. Thus, under conditions calling for less rotor thrust (and power) more power is available to the propellers, which can thus produce more thrust, largely counteracting the decreased rotor thrust.

For a buoyancy ratio substantially greater than unity, e.g. 1.39 as in Figure 2(c), the controllability is, surprisingly, greater than at maximum load ($\gamma = 0.61$). Inertial mass is less, and rotor thrust is approximately of the same magnitude in both cases, but for $\gamma > 1.0$ it is directed downward. Consequently the control mixing between roll (differential rotor thrust) and side force (vectoring of rotor thrust) must be reversed, so that the vehicle will be rolled "out of the wind", causing its downward rotor thrust to produce a component against the wind.

6.1.2 Longitudinal Acceleration

The three graphs grouped together as Figure 3 show linear acceleration capability in the longitudinal (X) direction as a function of wind speed for sideslip angles of 0, 20, 40, 60 and 90 degrees, and for several conditions of loading varying from minimum flying weight to maximum useful load. Figures 3(a), 3(b), and 3(c) show this capability for the same Heli-Stat versions, respectively, as do Figures 2(a), 2(b), and 2(c) for lateral acceleration, namely 21,200 m^3 (750,000 ft^3), 28,300 m^3 (1,000,000 ft^3), and 42,500 m^3 (1,500,000 ft^3).

As in the case of lateral acceleration, for each size aerostat longitudinal acceleration is also seen to decrease with decreasing buoyancy ratio, and increasing the aerostat volume leads to decreased acceleration, and for the same reason (increased inertial mass).

There are distinct differences, however, between Figures 2 and 3.

a) Longitudinal translation capability is consistently greater than lateral, and the ratio between them increases rapidly with wind speed. The reason for this is that aerodynamic drag in the transverse (lateral) direction for the total Heli-Stat is six to twelve times, dependent on fineness ratio, that in the longitudinal direction. Moreover the "additional apparent mass" representing the mass of surrounding air which must be accelerated is four to ten times as large laterally as longitudinally. The control forces available in the configurations analyzed, on the other hand, are approximately equal in the longitudinal and lateral directions.

b) For the lateral direction (Figure 2) the acceleration capability at zero degrees sideslip is independent of wind speed as a natural consequence of the fact that the drag has no lateral (Y) component. The equivalent case for longitudinal acceleration (Figure 3) is 90 degrees of sideslip, where the purely transverse drag has no longitudinal component. Hence in this case the longitudinal acceleration capability is independent of wind speed.

FIG. 3(a) HELI-STAT LONGITUDINAL ACCELERATION CAPABILITY IN HOVER VS. WIND SPEED

SEA LEVEL, 15°C (59°F.)

21,200 m^3 (750,000 Ft^3) AEROSTAT PLUS (4) SH-34 HELICOPTERS WITH TAIL ROTORS REPLACED BY 3.99 m (13 Ft) RING-TAILS

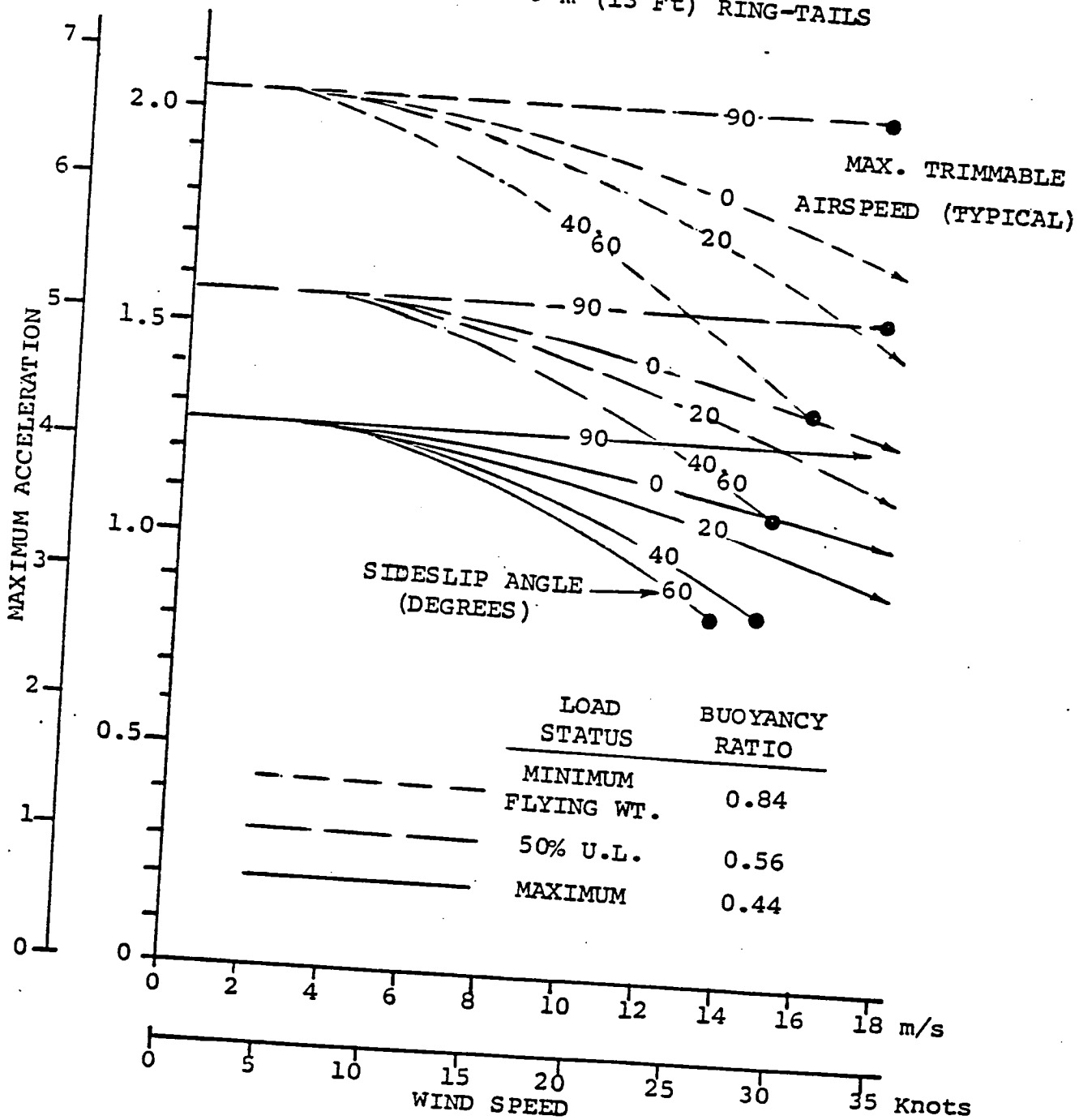

FIG. 3(b) HELI-STAT LONGITUDINAL ACCELERATION CAPABILITY IN HOVER VS. WIND SPEED (Cont'd)

SEA LEVEL, 15°C (59°F.)

28,300 m^3 (1,000,000 Ft^3) AEROSTAT PLUS (4) SH-34 HELICOPTERS WITH TAIL ROTORS REPLACED BY 3.99 m (13 Ft) RING-TAILS

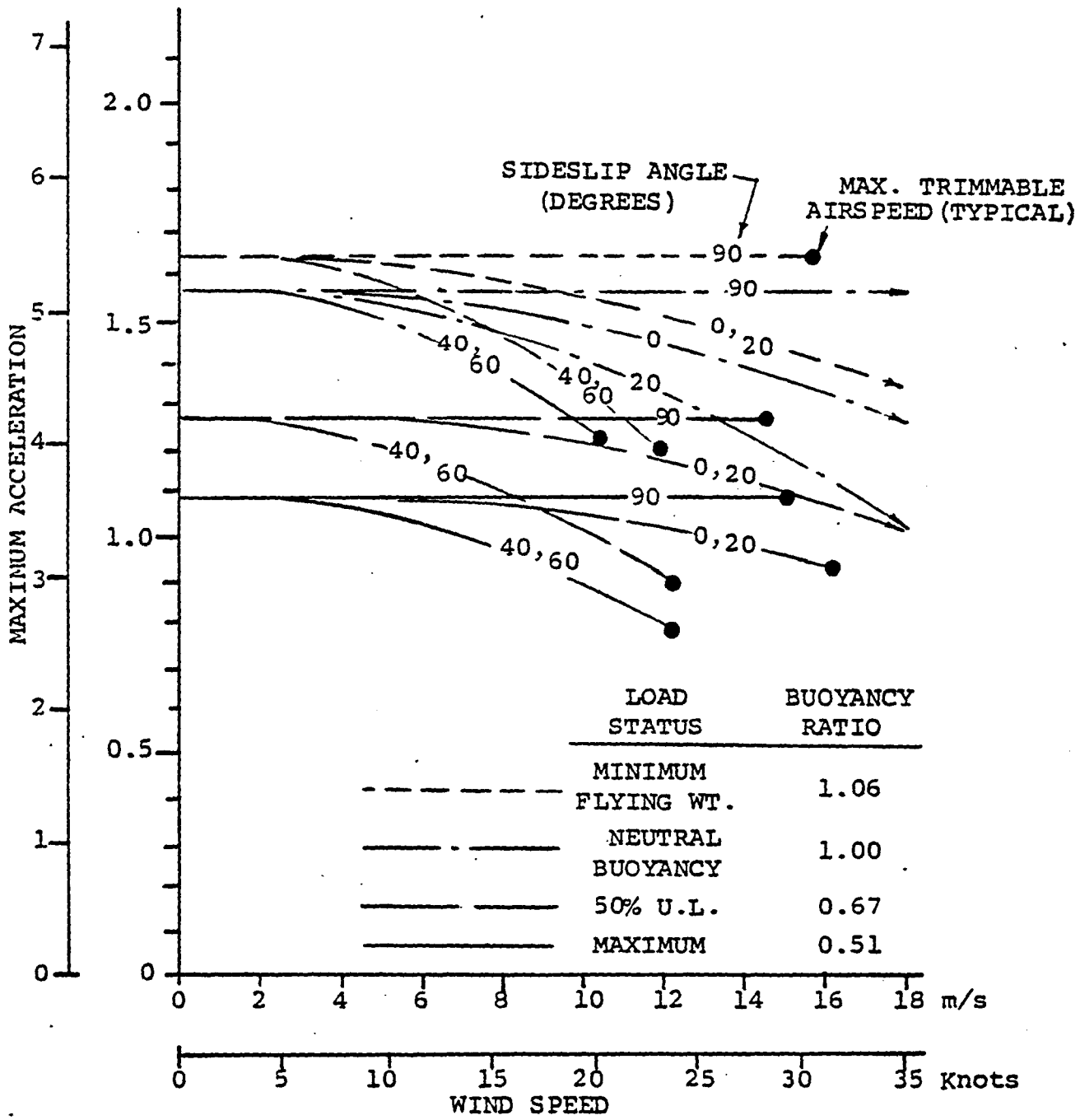

FIG. 3(c) HELI-STAT LONGITUDINAL ACCELERATION CAPABILITY IN HOVER VS. WIND SPEED (Cont'd)

SEA LEVEL, 15°C (59°F.)

42,500 m^3 (1,500,000 Ft^3) AEROSTAT PLUS (4) SH-34 HELICOPTERS WITH TAIL ROTORS REPLACED BY 3.99 m (13 Ft) RING-TAILS

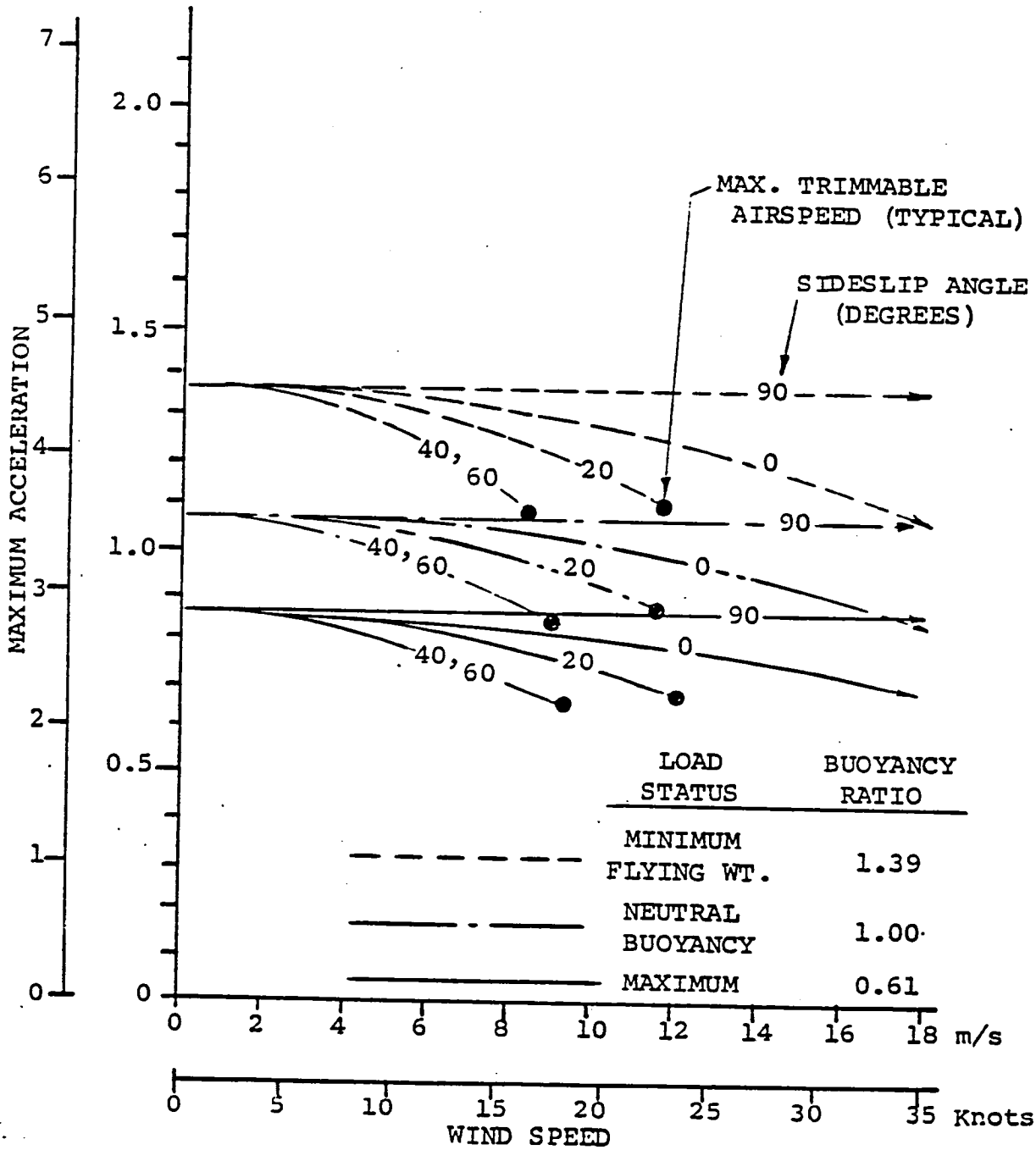

6.1.3 Yaw Acceleration

The three graphs grouped together as Figure 4 show angular acceleration capability in yaw as a function of wind speed for sideslip angles of 0, 20, 40, 60 and 90 degrees, and for the same conditions of loading as Figures 2 and 3. Figures 4(a), 4(b), and 4(c) show this capability for the same Heli-Stat versions, respectively, as do Figures 2(a), 2(b), and 2(c) for lateral acceleration, and the same as Figures 3(a), 3(b), and 3(c) for longitudinal acceleration, namely 21,200 m^3 (750,000 ft^3), 28,300 m^3 (1,000,000 ft^3), 42,500 m^3 (1,500,000 ft^3).

Yaw acceleration capability is affected in the same general way as is lateral or longitudinal with one notable exception. It is reduced by a significantly greater percentage with increased volume, reflecting the fact that yaw moment of inertia increases by the square of linear dimensions in addition to the effect of increased mass. Thus, comparing the acceleration capability of the 27,200 m^3 (750,000 ft^3) vehicle with the 42,500 m^3 (1,500,000 ft^3) vehicle at similar loading conditions, the longitudinal acceleration is reduced by an average of 31% and the lateral by an average of 46%, while yaw is reduced by an average of 68%, and up to 90% at the most critical sideslip angles.

FIG. 4(a) HELI-STAT YAW ACCELERATION CAPABILITY VS. WIND SPEED

SEA LEVEL, 15°C (59°F.)

21,200 m^3 (750,000 Ft^3) AEROSTAT PLUS

(4) SH-34 HELICOPTERS WITH TAIL ROTORS

REPLACED BY 3.99 m (13 Ft) RING-TAILS

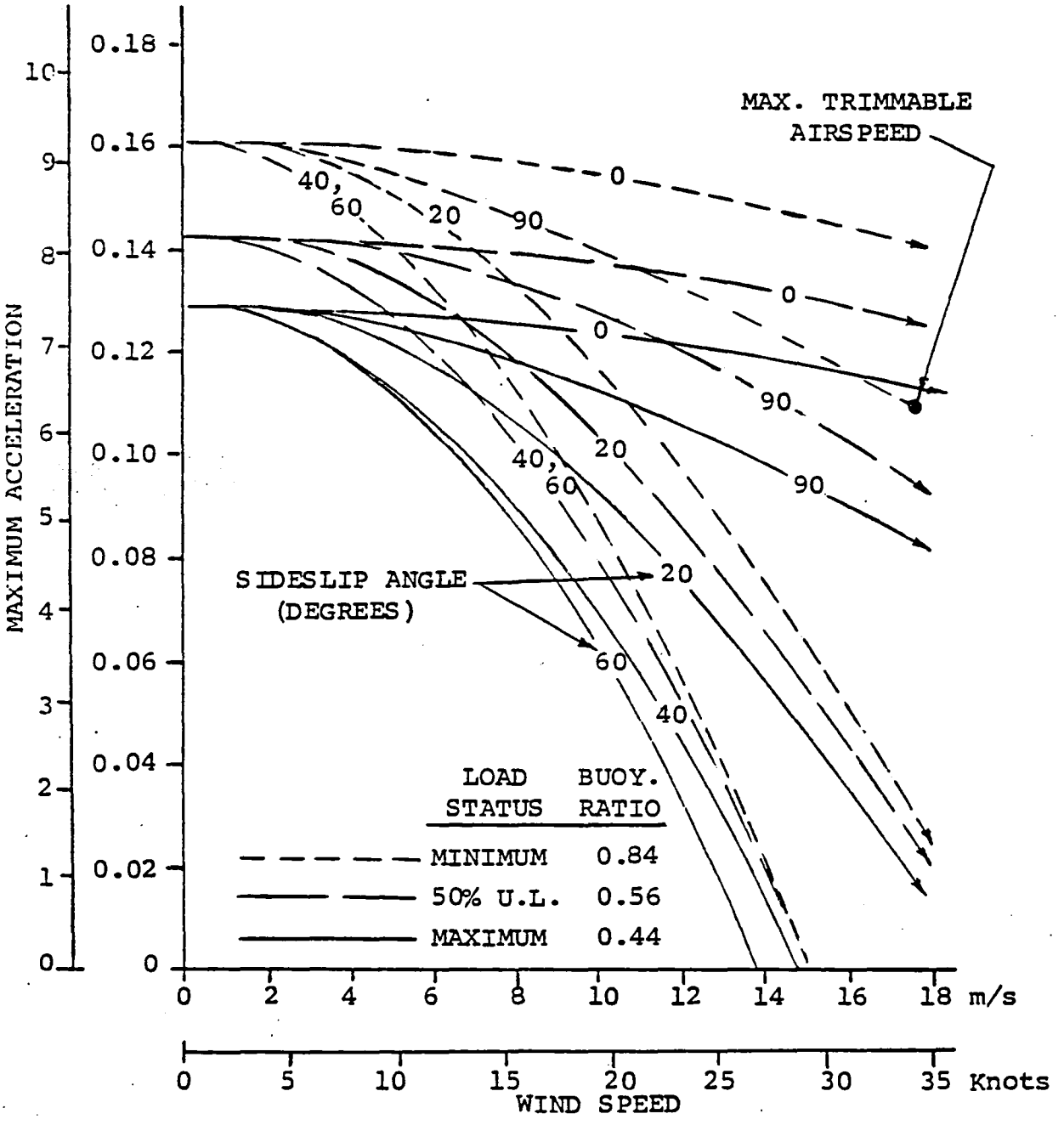

FIG. 4(b) HELI-STAT YAW ACCELERATION CAPABILITY VS. WIND SPEED (Cont'd)

SEA LEVEL, 15°C (59°F.)

28,300 m^3 (1,000,000 Ft^3) AEROSTAT PLUS (4) SH-34 HELICOPTERS WITH TAIL ROTORS REPLACED BY 3.99 m (13 Ft) RING-TAILS

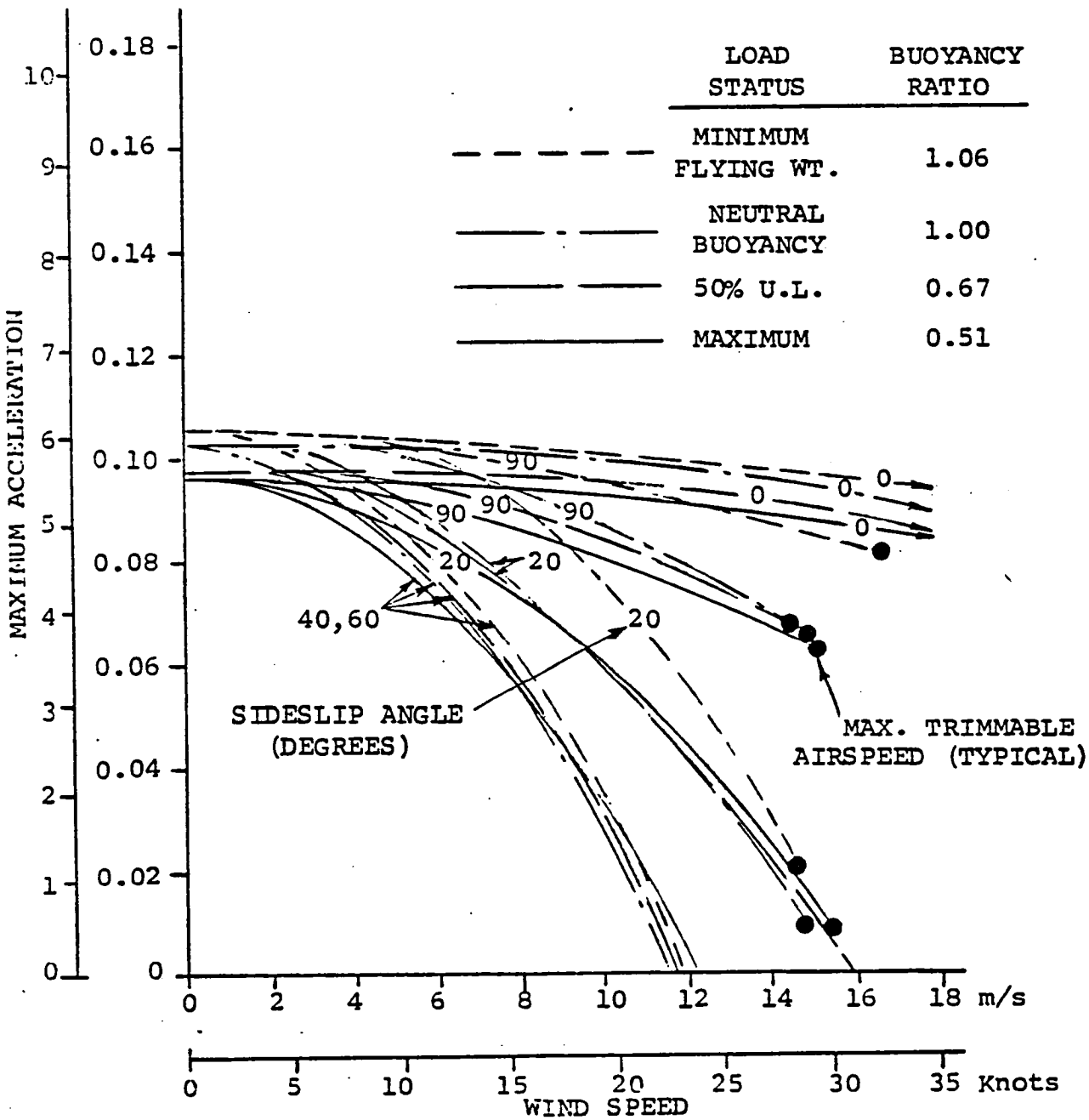

FIG. 4(c) HELI-STAT YAW ACCELERATION CAPABILITY VS. WIND SPEED (Cont'd)

SEA LEVEL, 15°C (59°F.)

42,500 m^3 (1,500,000 Ft^3) AEROSTAT PLUS (4) SH-34 HELICOPTERS WITH TAIL ROTORS REPLACED BY 3.99 m (13 Ft) RING-TAILS

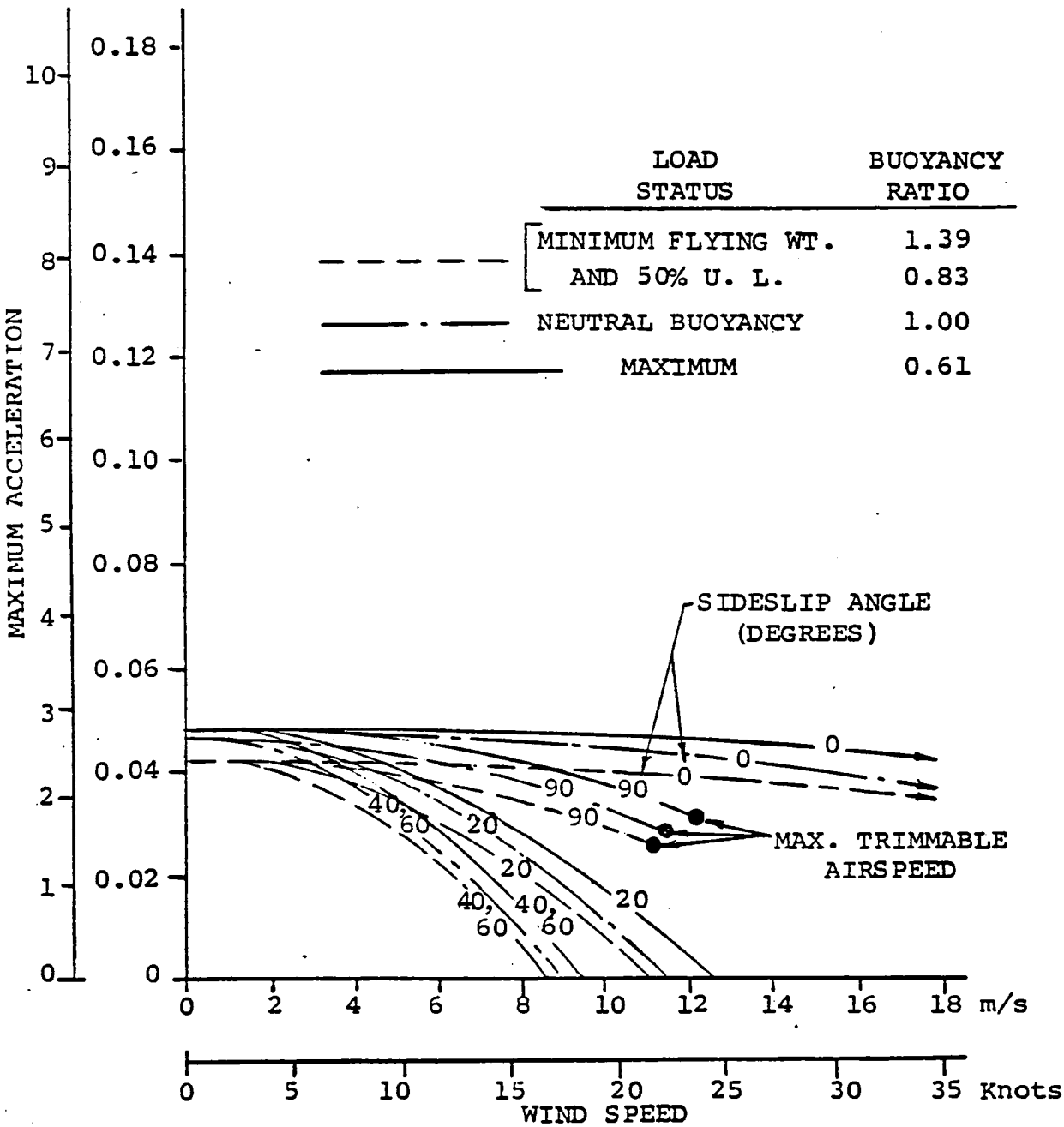

6.2 MAXIMUM TRIMMED AIRSPEED IN CROSSWINDS

Figures 5(a), (b) and (c) show the maximum airspeed to which each of the three Heli-Stat sizes can be trimmed as a function of sideslip angle, and for buoyancy ratios corresponding to a range, for each size, from minimum flying weight to maximum weight. These graphs were constructed from the graphs of Figures 3 and 4, using the values of wind speed at which acceleration capability becomes zero.

In general the most critical sideslip angles are in the region from 40 to 70 degrees. This is to be expected, since the aerodynamic yawing moment on an ellipsoidal body is proportional to the sine squared of the sideslip angle, which is maximum at 45 degrees.

Comparing Figures 5(a), (b), and (c) against each other shows that the controllability, as measured by crosswind capability, varies more with aerostat size (volume) than with load variation in a given size. In the 28,300 m^3 (1,000,000 ft^3) size, Figure 5(b), the Heli-Stat can hover in a 45-degree sideslip in winds of 11 to 11.5 m/s (21 to 22.5 knots) at all buoyancy ratios to which it can be loaded.

Figure 5(a), for the 21,200 m^3 (750,000 ft^3) aerostat, shows the same trends as Figure 5(b) except that, because of its smaller buoyant volume, it cannot be flown in a condition approaching neutral buoyancy, even at minimum flying weight. Since the dynamic thrusters can produce the same moments as for the larger 28,300 m^3 (1,000,000 ft^3) Heli-Stat, while the aerodynamic drag and yawing moment of the smaller aerostat are smaller, this smaller size is seen to be more maneuverable, and can resist a 45-degree cross wind up to at least 13.5 m/s (26 knots) at all loading conditions.

On the other hand, the still larger 42,500 m^3 (1,500,000 ft^3) Heli-Stat is less maneuverable, having a 45-degree sideslip capability in wind up to about 8.5 m/s (16 knots). At minimum flying weight this version, when inflated 95.0% with helium, has positive buoyancy (1.39 buoyancy ratio). It requires negative rotor thrust for vertical trim, and reversed control mixing between differential rotor thrust and rotor thrust vectoring, as explained in Section 6.1.1. With this change in control mixing, however, it is as controllable as when fully loaded.

FIG. 5(a) MAX. TRIMMED HELI-STAT AIRSPEED VS. SIDESLIP ANGLE FOR VARYING BUOYANCY RATIO (B)

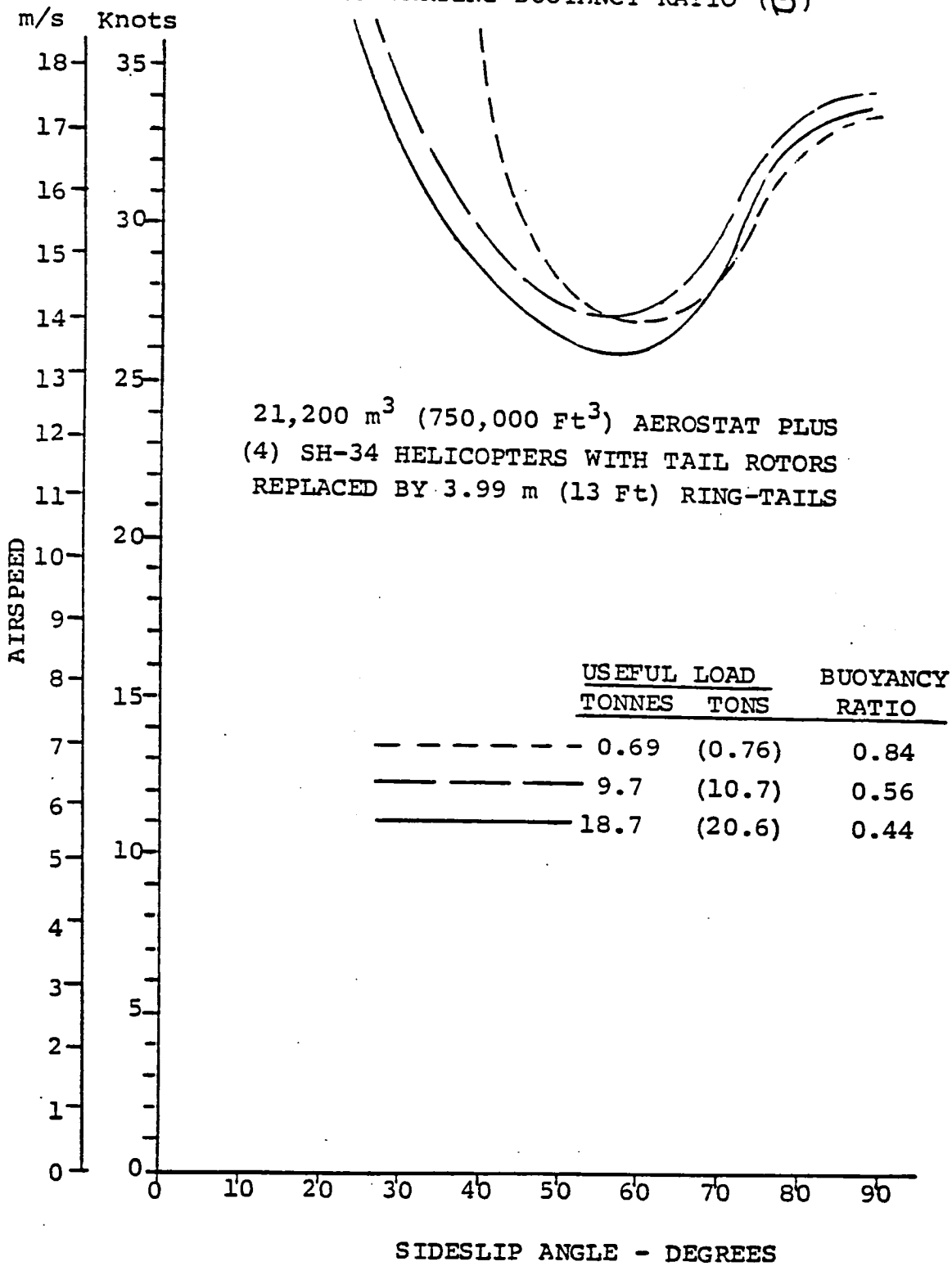

21,200 m^3 (750,000 Ft^3) AEROSTAT PLUS (4) SH-34 HELICOPTERS WITH TAIL ROTORS REPLACED BY 3.99 m (13 Ft) RING-TAILS

USEFUL LOAD TONNES	USEFUL LOAD TONS	BUOYANCY RATIO
0.69	(0.76)	0.84
9.7	(10.7)	0.56
18.7	(20.6)	0.44

FIG. 5(b) MAX. TRIMMED HELI-STAT AIRSPEED VS. SIDESLIP ANGLE FOR VARYING BUOYANCY RATIO (β) (Cont'd)

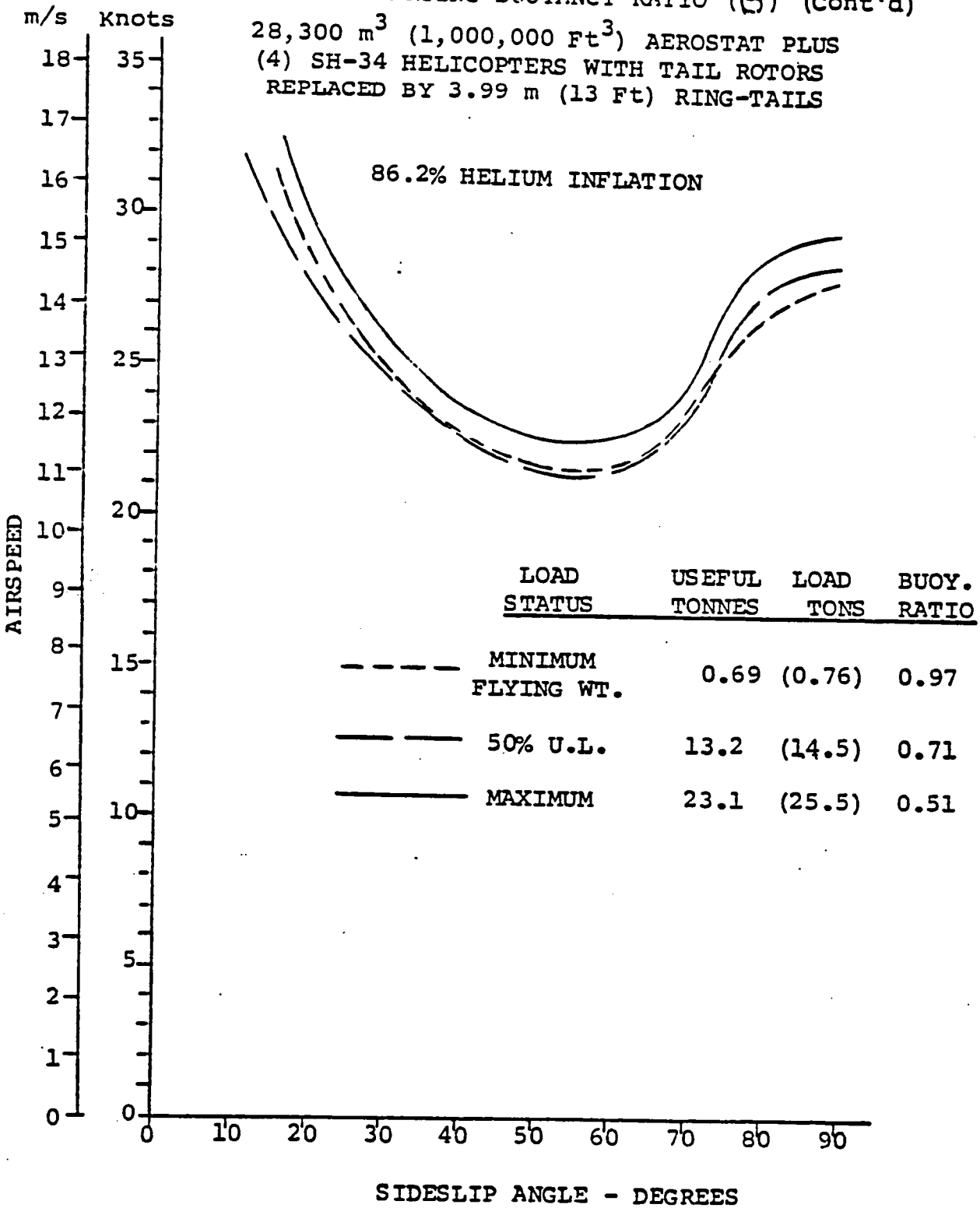

FIG. 5(c) MAX. TRIMMED HELI-STAT AIRSPEED VS. SIDESLIP ANGLE FOR VARYING BUOYANCY RATIO (β) (Cont'd)

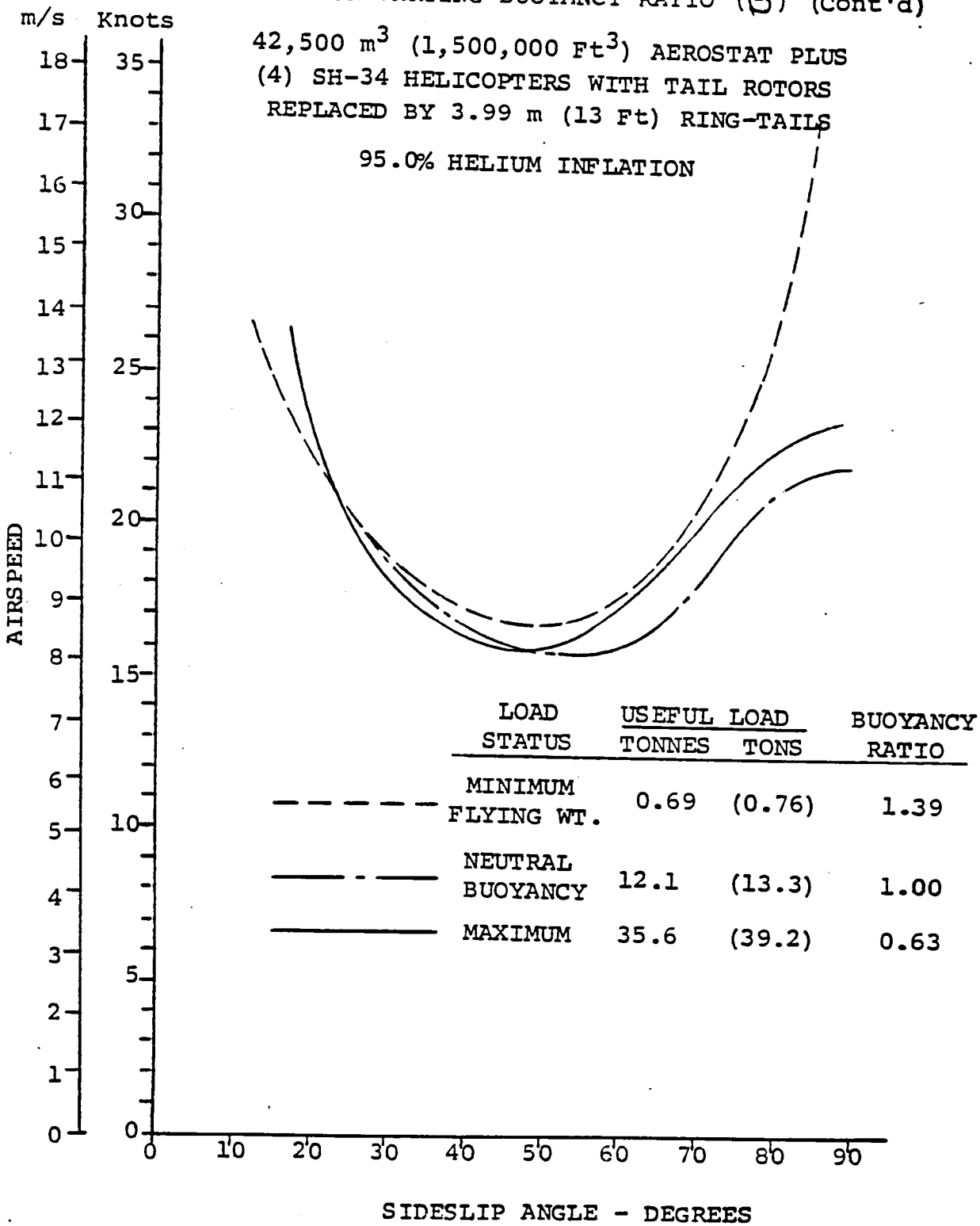

LOAD STATUS	USEFUL LOAD TONNES	USEFUL LOAD TONS	BUOYANCY RATIO
MINIMUM FLYING WT.	0.69	(0.76)	1.39
NEUTRAL BUOYANCY	12.1	(13.3)	1.00
MAXIMUM	35.6	(39.2)	0.63

6.3 CROSSWIND HOVER CAPABILITY VS. USEFUL LOAD

Figures 3(a), (b), (c), and (d) show the maximum wind speed against which the three sizes of Heli-Stat can be hovered, as a function of useful load, at sideslip angles of 20, 40, 60, and 90 degrees, respectively. These four figures are similar in that they clearly show that the controllability, as measured by crosswind hover capability, for a series of different size aerostats, all with the same system of dynamic thrusters (including spacing), is a decreasing function of aerostat volume at all sideslip angles. Note that Figure 3(a) (20-degree sideslip) shows graphs for only the two largest volumes. The graph for the 21,200 m^3 (750,000 ft^3) size would lie completely above the maximum wind speed shown in the figure, as can be verified by referring to Figure 2(a).

The variation in controllability for each size depends on useful load to only a minor degree. This is also implied in Figures 2(a), (b), and (c) which all show a "clustering" of the graphs for different buoyancy ratios.

As useful load is decreased further, producing a loading condition involving negative (downward) dynamic lift ($\beta > 1.0$), downward rotor thrust can be vectored as effectively as the more normal upward thrust. However, the control mixing between lateral differential thrust (roll control) and lateral thrust vectoring must be reversed for this condition of buoyancy ratio greater than one as explained in Section 6.1.1.

6.4 DISCUSSION

The calculated acceleration capability for a given wind speed and sideslip angle will be lower when the lift induced on the aerostat at an angle of sideslip is included in the static trim equations. This would reduce the maximum trimmable airspeed by a calculated amount of 1 to 3 knots at a 40 degree sideslip angle. Including stability effects, not part of this scope of work, would reduce this apeed by an estimated additional 1 to 3 knots.

FIG. 6(a) HELI-STAT MAXIMUM CROSS-WIND HOVER CAPABILITY VS.USEFUL LOAD

SEA LEVEL, 15°C (59°F.)

(4) SH-34 HELICOPTERS WITH TAIL ROTORS REPLACED BY 3.99 m (13 Ft) RING-TAILS

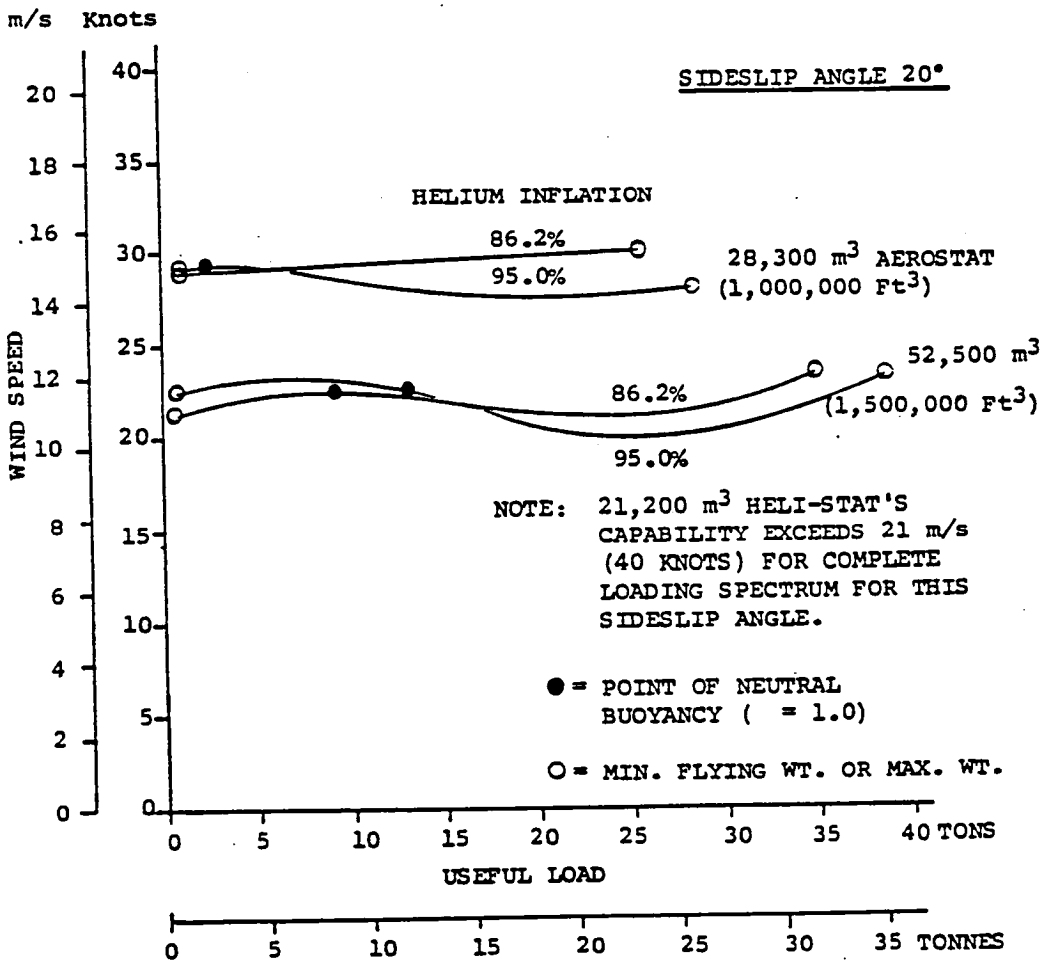

FIG. 6(b) HELI-STAT MAXIMUM CROSS-WIND HOVER CAPABILITY VS.USEFUL LOAD

SEA LEVEL, 15°C (59°F.)

(4) SH-34 HELICOPTERS WITH TAIL ROTORS REPLACED BY 3.99 m (13 Ft) RING-TAILS

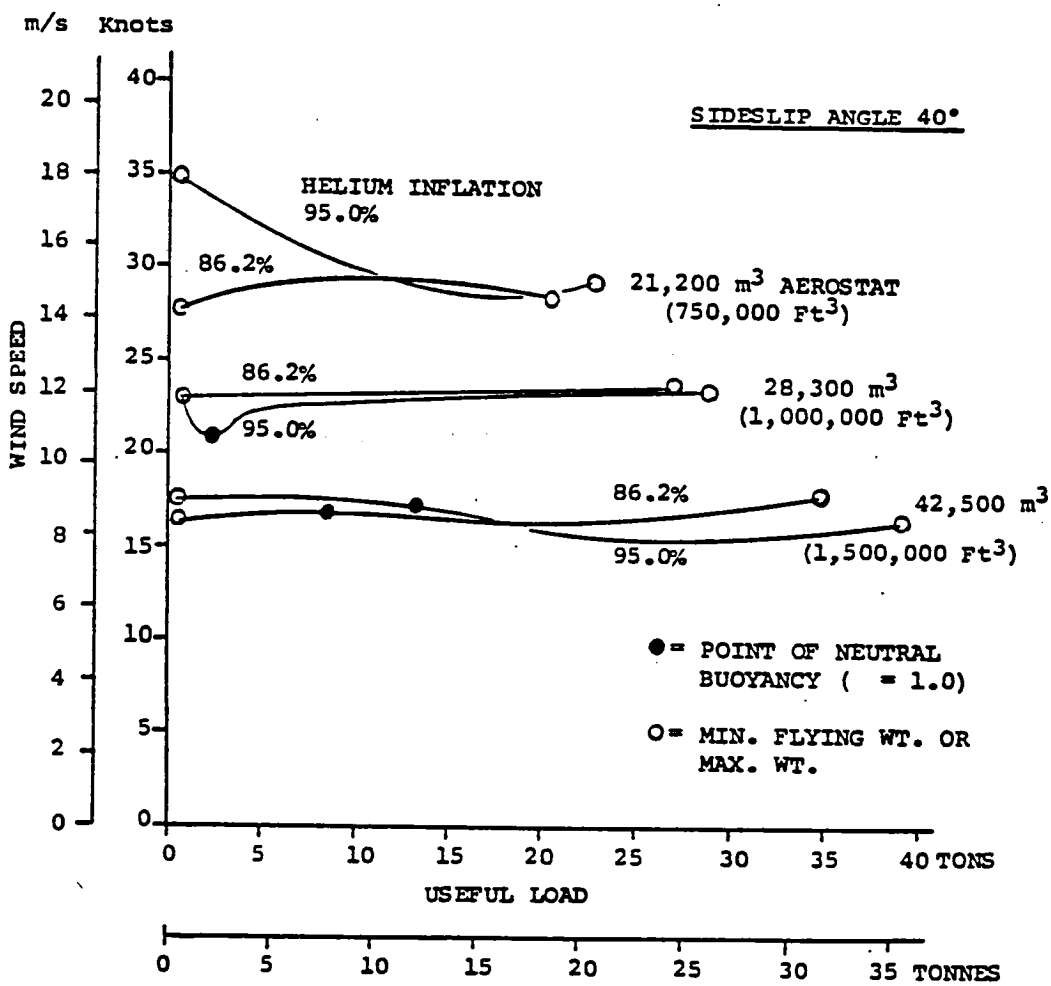

FIG. 6(c) HELI-STAT MAXIMUM CROSS-WIND HOVER CAPABILITY VS.USEFUL LOAD (Cont'd)
SEA LEVEL, 15°C (59°F.)

(4) SH-34 HELICOPTERS WITH TAIL ROTORS REPLACED BY 3.99 m (13 Ft) RING-TAILS

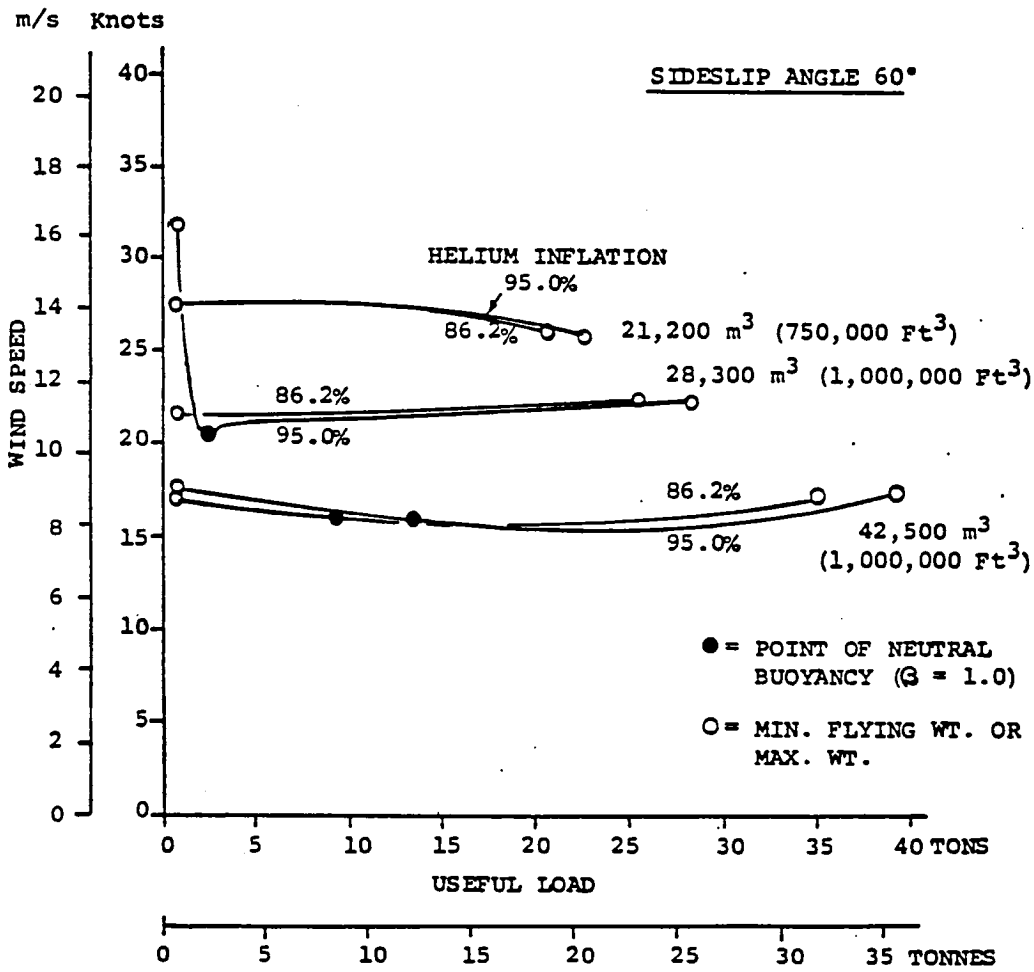

FIG. 6(d) HELI-STAT MAXIMUM CROSS-WIND HOVER CAPABILITY VS. USEFUL LOAD

SEA LEVEL, 15°C (59°F.)

(4) SH-34 HELICOPTERS WITH TAIL ROTORS REPLACED BY 3.99 m (13 Ft) RING-TAILS

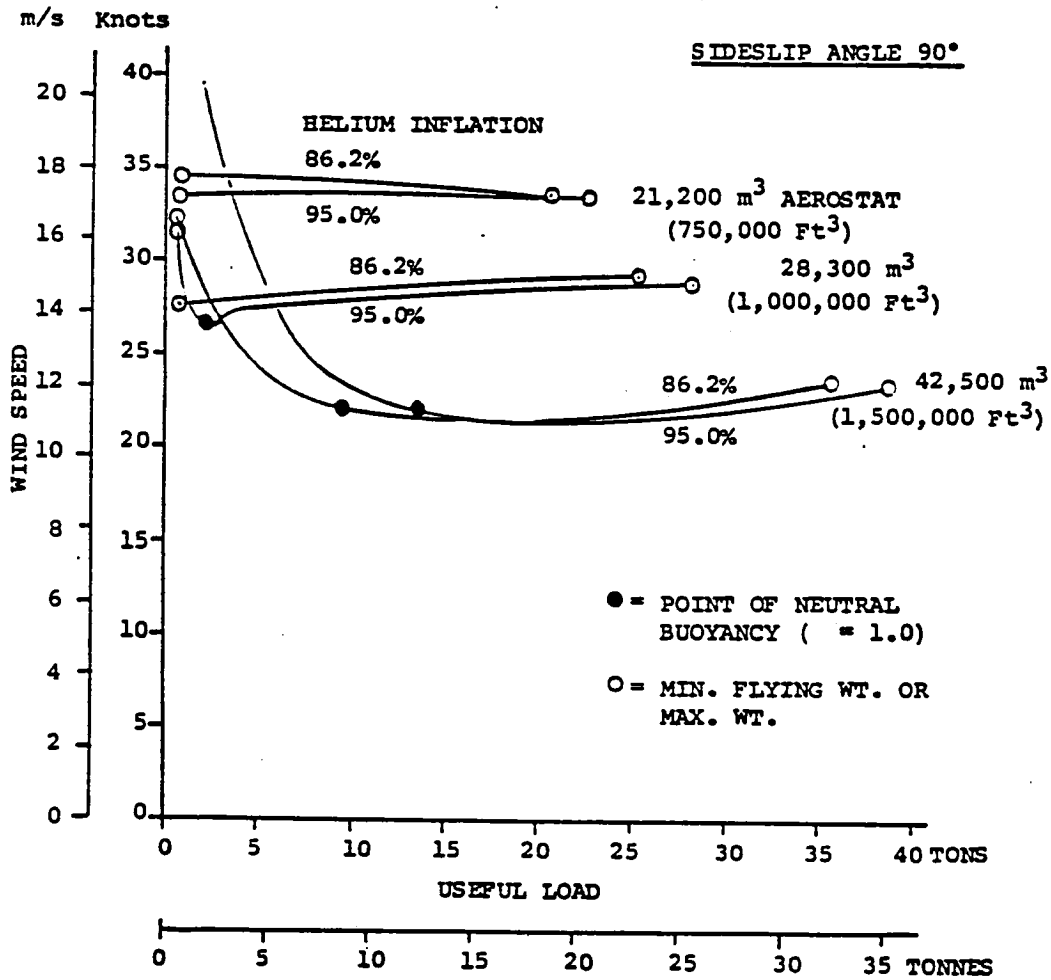

7. CONCLUSIONS

1. Horizontal thruster(s) capable of producing lateral forces are desirable under conditions of near neutral buoyancy. As buoyancy ratio departs from this value, in either direction, the importance of lateral thrusters decreases.

2. For vehicles with varying sizes of aerostats but the same configuration of dynamic thrusters, the controllability, as measured by acceleration capability, decreases with increasing aerostat volume, especially in yaw because of the increased moment of inertia.

3. The ability to roll the vehicle increases significantly the ability to trim and accelerate a hybrid LTA vehicle in a crosswind.

4. For loading conditions when buoyancy ratio is greater than one, the control mixing between roll and lateral vectoring must be reversed.

8. REFERENCES AND BIBLIOGRAPHY

NO.	REPORT NO.	CO. OR AGENCY	TITLE	AUTHOR	DATE
1.	97-X-11	Piasecki Aircraft	"Design Feasibility Analysis, Ultra-Heavy Vertical Lift System - The Heli-Stat"		24 June 76
2.			"Fluid Dynamic Drag"	S.F.Hoerner	1958
3.	Vol. VI	Dover Publications, Inc. New York, N.Y.	"Aerodynamic Theory"	W.F.Durand	1963
4.	405	NACA	"Application of Practical Hydrodynamics to Airship Design"	Upson and Klikoff	1931
5.	AFFT6-TR-56-8	ARDC USAF	"H-34A Phase IV - Performance Test"	W.J.Chabot	May, 1956
6.	PiAC 97-C-1 NADC 76327-30	PiAC for NADC	"Hybrid LTA Vehicle Controllability as affected by Thruster Magnitude and Spacing"	Meyers et al	1 July 77

9. ABBREVIATIONS AND SYMBOLS

Symbols	Definition	Units S.I.	Units Customary
a	acceleration, linear	m/s^2	$ft./sec.^2$
C.B.	center of buoyancy		
C.G.	center of gravity		
C_D	drag coefficient, based on $\forall^{2/3}$		
C_L	lift coefficient, based on $\forall^{2/3}$		
C_M	moment coefficient, based on $\forall$		
℄	center-line		
D	drag force	N	lb(f)
D	diameter	m	ft.
deg.	degrees	deg.	deg.
f.r.	fineness ratio (length/diameter)		
g	acceleration of gravity	m/s^2	$ft./sec.^2$
G.W.	gross weight	kg.	lb(m)
H_{CG}	height of vehicle center of gravity (defined in Fig. 7)	m	ft.
H_{RTR}	height of main rotors (defined in Fig. 7)	m	ft.
I_X, I_Y, I_Z	mass moment of inertia about X, Y and Z axes (roll, pitch, and yaw, respectively)	$kg.m^2$	slug $ft.^2$

9. ABBREVIATIONS AND SYMBOLS (Cont'd)

Symbols	Definition	Units S.I.	Units Customary
k_1	coefficient of additional apparent mass for longitudinal motion, equals additional apparent mass divided by actual mass		
k_2	coefficient of additional apparent mass for transverse motion, defined as above		
L	lift	N	lb.
L	rolling moment	N.m	lb.-ft.
L	overall length	m	ft.
L_B	total buoyant lift (weight of displaced volume of air), thus equal to $g\rho\forall$	N	lb.
L_{CW}	crosswind "lift" force		
m	mass	kg.	slugs
N	yawing moment	N.m	lb.-ft.
N	Newton - international unit of force, equals 0.2248 lb.		
q	dynamic pressure = $1/2\,\rho\,v^2$	N/m^2	$lb./ft.^2$
R	radius	m	ft.
S	area	m^2	$ft.^2$
T	thrust	N	lb.
t	time	s	sec.
T_R	average thrust of each lifting rotor; i.e. when $\Delta T_Z = 0$	N	lb.

9. ABBREVIATIONS AND SYMBOLS (Cont'd)

Symbols	Definition	Units S.I.	Units Customary
T_{P_X}	X component of horizontal thrusters (defined in Fig. 7)	N	lb.
T_{P_Y}	Y component of horizontal thrusters (defined in Fig. 7)	N	lb.
V	flight path velocity	m/s	ft./sec. or knots
v	sideslip velocity	m/s	ft./sec.
$\forall$	volume	m^3	$ft.^3$
W	weight (in vacuum) of entire mass of vehicle, including internal gases	N	lb.
X	direction of longitudinal axis		
x	displacement in X direction	m	ft.
X_{RTR}	rotor longitudinal spacing (defined in Fig. 7)	m	ft.
Y	direction of lateral axis		
y	displacement in Y direction (lateral)	m	ft.
Y_{RTR}	rotor lateral spacing (defined in Fig. 7)	m	ft.

9. ABBREVIATIONS AND SYMBOLS (Cont'd)

Symbols	Definition	Units S.I.	Units Customary
α	angular acceleration	rad./s^2	rad./$sec.^2$
β	sideslip angle (wind angle, Fig. 7)	deg.	deg.
β	buoyancy ratio (static lift/total lift)		
ΔT_Z	differential thrust of lifting rotors (each) for roll or pitch control	N	lb.
γ_X, γ_Y	vectoring of main rotor thrust in X or Y direction (defined in Fig. 7)	deg.	deg.
ρ	air density	kg/m^3	$slugs/ft.^3$
ϕ	roll angle	deg.	deg.
ψ	yaw angle	deg.	deg.
$\dot{(\ )}$	first time derivative of ( )		
$\ddot{(\ )}$	second time derivative of ( )		

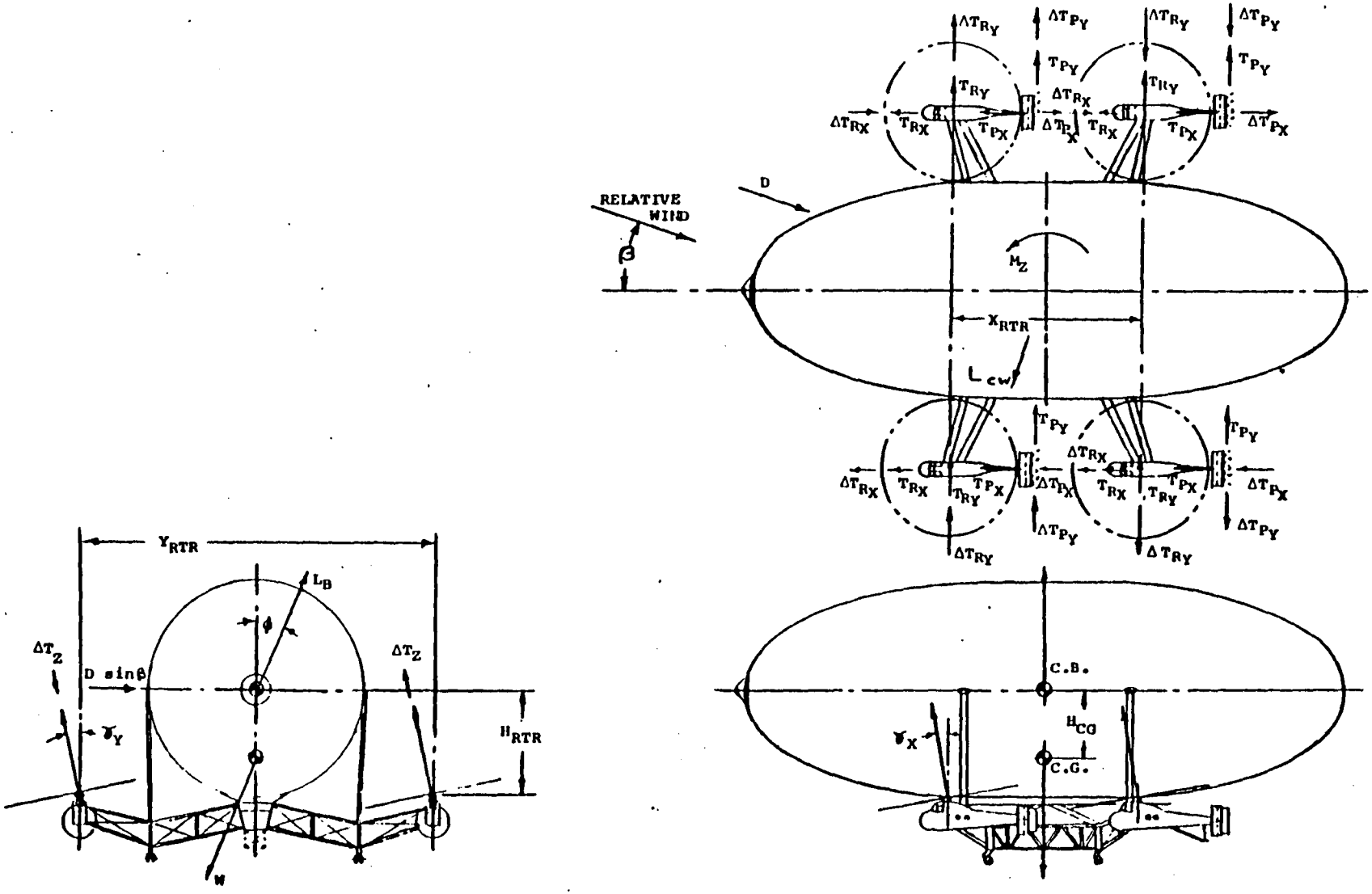

FIG. 7 FORCES ON TRIMMED VEHICLE

DATA FROM REF. 2, "AERODYNAMIC DRAG" BY HOERNER

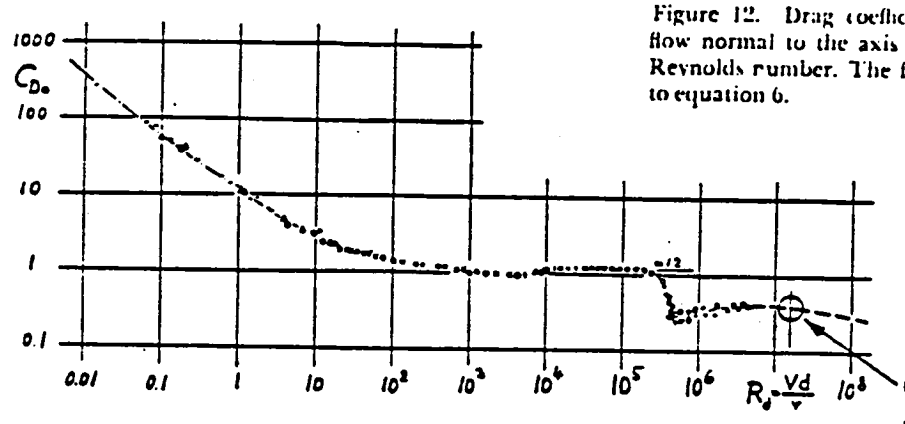

Figure 12. Drag coefficient of the circular cylinder in a flow normal to the axis (between walls), as a function of Reynolds number. The function below R = 1, corresponds to equation 6.

C_D = 0.39 used for cyl. portion of aerostat at = 90°

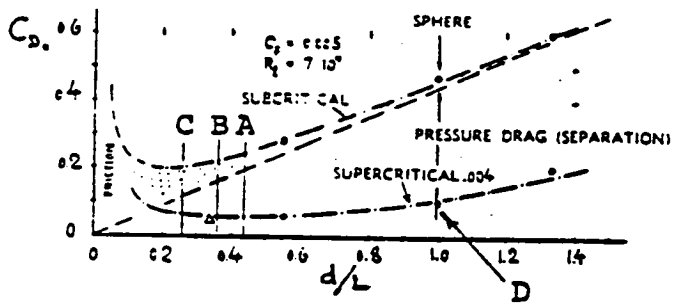

Figure 19. Drag coefficients of ellipsoidal bodies (22); (a) at a subcritical Reynolds number R_l = 7 10^6; and (b) above transition, at R'numbers approaching 10^6).

AEROSTAT AT β = 0°		
	Vol. (m^3)	C_D
A	21,200	.055
B	28,300	.055
C	42,500	.060

D "Spherical" ends of aerostat at β = 90°. C_D = 0.115

Figure 10. Profile drag coefficients of symmetrical wing and strut sections, based on frontal area, as a function of chord thickness ratio.

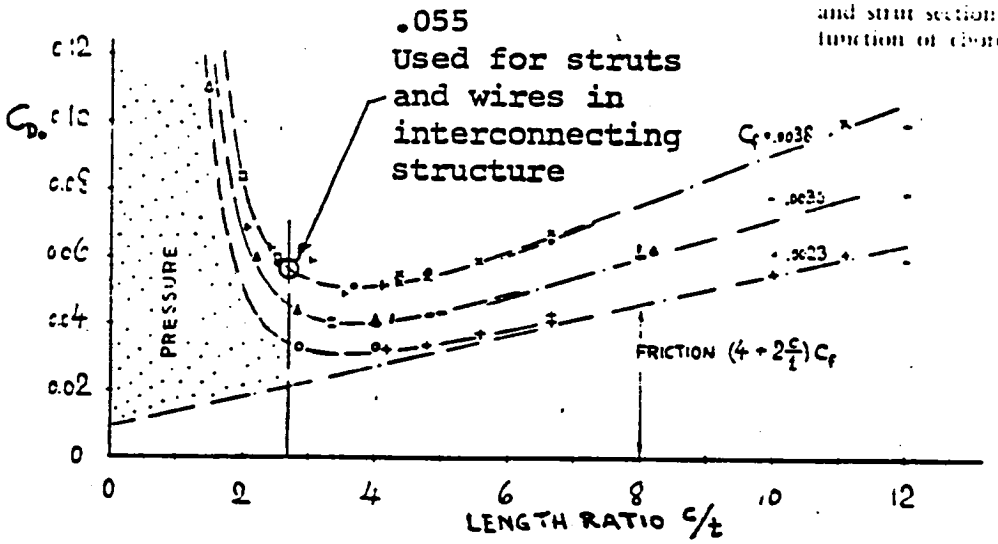

DATA FROM REF. 4, NACA REPORT 405,
"APPLICATION OF PRACTICAL HYDRODYNAMICS TO AIRSHIP DESIGN"

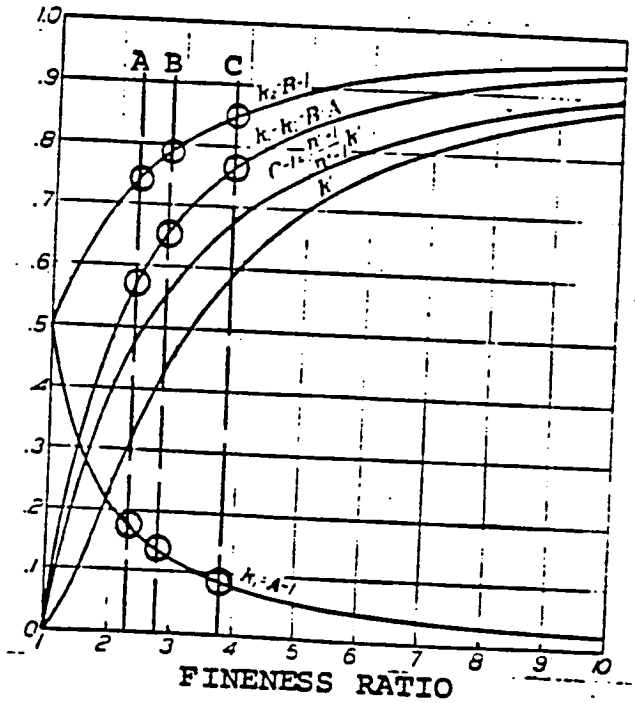

FIGURE 1. INERTIA COEFFICIENTS OF ELLIPSOIDS

	Vol. (m^3)	K_1	K_2	K_2-K_1
A	21,200	0.17	0.72	0.55
B	28,300	0.19	0.79	0.66
C	42,500	0.08	0.85	0.77

If the moment is taken around the center of volume, the last term disappears, making the total moment for either circular or pitched flight:

$$M_0 = q(k_2 - k_1)\ (\text{vol})\ \sin 2\psi_0. \qquad (7)$$

This is Equation 2 of Report, used in yaw trim analysis.

1. Report No.	2. Government Accession No.	3. Recipient's Catalog No.
NASA CR -152344		

4. Title and Subtitle	5. Report Date
Hybrid LTA Vehicle Controllability As Affected By Buoyancy Ratio	October 24, 1979
	6. Performing Organization Code
7. Author(s) Donald N. Meyers, Piotr Kubicki, T. Tarczynski, A. Fairbanks, F. N. Piasecki	8. Performing Organization Report No. PiAC Rpt. No.97-C-6
9. Performing Organization Name and Address Piasecki Aircraft Corporation Island Rd., International Airport Philadelphia, PA 19153	10. Work Unit No.
	11. Contract or Grant No. NAS2-10185
12. Sponsoring Agency Name and Address National Aeronautics & Space Administration Washington, D.C. 20546	13. Type of Report and Period Covered Final Report
	14. Sponsoring Agency Code

15. Supplementary Notes

Technical Monitor - Peter D. Talbot
(415) 965-5887 or FTS 448-5887

16. Abstract

This report constitutes an investigation of the zero- and low-speed controllability of heavy-lift airships under various wind conditions as affected by the buoyancy ratio. A series of three hybrid LTA vehicles were examined, each having a dynamic-thrust system comprised of four H-34 helicopters, but with buoyant envelopes of different volumes (and hence buoyancies), and with varying percentage of helium inflation and varying useful loads (hence gross weights). Buoyancy ratio, B, was thus examined varying from approximately 0.44 to 1.39. For values of B greater than 1.0, the dynamic thrusters must supply negative thrust (i.e. downward).

17. Key Words (Suggested by Author(s))	18. Distribution Statement
LTA Vehicle, Heli-Stat, Buoyancy Ratio, Piasecki	Unclassified - Unlimited

19. Security Classif. (of this report)	20. Security Classif. (of this page)	21. No. of Pages	22. Price*
Unclassified	Unclassified	63	

*For sale by the National Technical Information Service, Springfield, Virginia 22161